Fall 2004

Coastal Change and Beach Ridges along the Northwest Coast of Peru: Image and GIS Analysisof the Chira, Piura, and Colán Beach-Ridge Plains

Stacy Shafer Rogers

Daniel H. Sandweiss
University of Maine, dan.sandweiss@umit.maine.edu

Kirk A. Maasch

Daniel F. Belknap

Peggy Agouris

Journal of Coastal Research	20	4	1102–1125	West Palm Beach, Florida	Fall 2004

Coastal Change and Beach Ridges along the Northwest Coast of Peru: Image and GIS Analysis of the Chira, Piura, and Colán Beach-Ridge Plains

Stacy Shafer Rogers†,††, Daniel H. Sandweiss†,‡, Kirk A. Maasch†,§, Daniel F. Belknap†,§, and Peggy Agouris*

†Climate Change Institute
University of Maine
Orono, ME 04469, USA

‡Department of Anthropology
University of Maine
Orono, ME 04469, USA

§Department of Earth Sciences
University of Maine
Orono, ME 04469, USA

*Department of Spatial Information Science and Engineering
University of Maine
Orono, ME 04469, USA

††Earth Tech
Concord, MA 01742, USA

ABSTRACT

ROGERS, S.S.; SANDWEISS, D.H.; MAASCH, K.A.; BELKNAP, D.F., and AGOURIS, P., 2004. Coastal change and beach ridges along the northwest coast of Peru: image and GIS analysis of the Chira, Piura, and Colán beach ridge plains. *Journal of Coastal Research,* 20(4), 1102–1125. West Palm Beach (Florida). ISSN 0749-0208.

Since approximately 5200 cal yrs BP, five sets of eight to nine beach ridges were built and preserved along the northwestern Peruvian coastal desert (3°30′S–9°S). Potential ridge-building mechanisms in the hyper-arid environment of northwest Peru include El Niño floods and storms, seismic activity, and sea-level change, as well as more gradual climate changes that affected coastal morphology. Image processing and Geographic Information System (GIS) methods were used to analyze aerial photographs and measure historic coastal patterns along three beach-ridge plains over a 37-year time period. Coastal features were digitized from image mosaics of each ridge plain at different time intervals from 1946 up to 1983. Progradation rates were examined at ridge locations north of the Chira River and Piura River, as well as at the base of ephemeral stream valleys in Colán. The total change in beach area was measured from historic aerial photographs taken at different time intervals. The resulting measurements showed that sediment distributed by El Niño storms was redeposited along the shoreline within a few years following each event. The difference between the frequency of El Niño events (currently 2–7 years) and the rate of ridge preservation (1 per 500 years average) suggests that individual ridges may be composites of multiple depositional events, or that ridges result from the rare convergence of multiple processes and conditions. A change in style of ridge formation in all studied beach-ridge sets correlates with, and may be explained by, change in the frequency of El Niño events at about 3000 cal yrs BP.

ADDITIONAL INDEX WORDS: *El Niño, ENSO, beach ridge, coastal change, Geographic Information Systems, GIS, image processing, Peru, geoarchaeology.*

INTRODUCTION

On a cycle of 2–7 years, Peru's hyperarid coast experiences extreme precipitation during the El Niño phase of El Niño/Southern Oscillation (ENSO) events. ENSO results from naturally occurring interannual variability in the Pacific ocean-atmosphere system. Reconstructing the history of El Niño in South America can help to evaluate past cultural changes and infer the potential future effects of ENSO activity (RICHARDSON, 1983; MOSELEY *et al.,* 1992; SANDWEISS *et al.,* 2001). Climate variability can significantly affect human culture and survival (ENFIELD, 1992). Four beach-ridge plains on the desert coast of northwestern Peru were apparently built by El Niño activity: Chira, Colán, Piura, and Santa (MOSELEY *et al.,* 1992; ORTLIEB *et al.,* 1993; ORTLIEB and MACHARÉ, 1993; ORTLIEB *et al.,* 1995; RICHARDSON, 1983; SANDWEISS *et al.,* 1983, 1998; SANDWEISS, 1986) (Figure 1). A fifth beach-ridge plain at Tumbes on the Peru-Ecuador border has not been studied in detail. All of these plains formed during the late Holocene, and each set contains eight to nine ridges. The oldest ridge at all the locations dates to approximately 5200 cal yrs BP (RICHARDSON, 1983; SANDWEISS, 1986; ORTLIEB *et al.,* 1993; ORTLIEB *et al.,* 1995).

Beach ridges are raised linear features that form parallel to the coast and mark previous coastline positions. In northwest Peru, prograding ridge sequences occur within coastline segments that demonstrate a log-spiral, or zeta form (DAVIES, 1980). Headlands cause large-scale refraction that influences longshore currents, but episodic beach-ridge formation requires additional processes. In general, beach ridges prograde at the foreshore whenever longshore currents bring more material to the beach than local wave activity can remove. As new sand or gravel is accreted to the shore, the old beachface is abandoned and may be preserved as a ridge. Climate, sea level, wave height, and sediment-supply fluctuations control the orientation, elevation, and morphology of beach-ridge plains (TAYLOR and STONE, 1996). Changes in these environmental conditions can result in interruptions, truncations, or erosion of previous ridge features, which may be followed by the deposition of younger beach ridges with different orientations or shapes (TAYLOR and STONE, 1996).

03-0006R received and accepted in revision 21 August 2003.

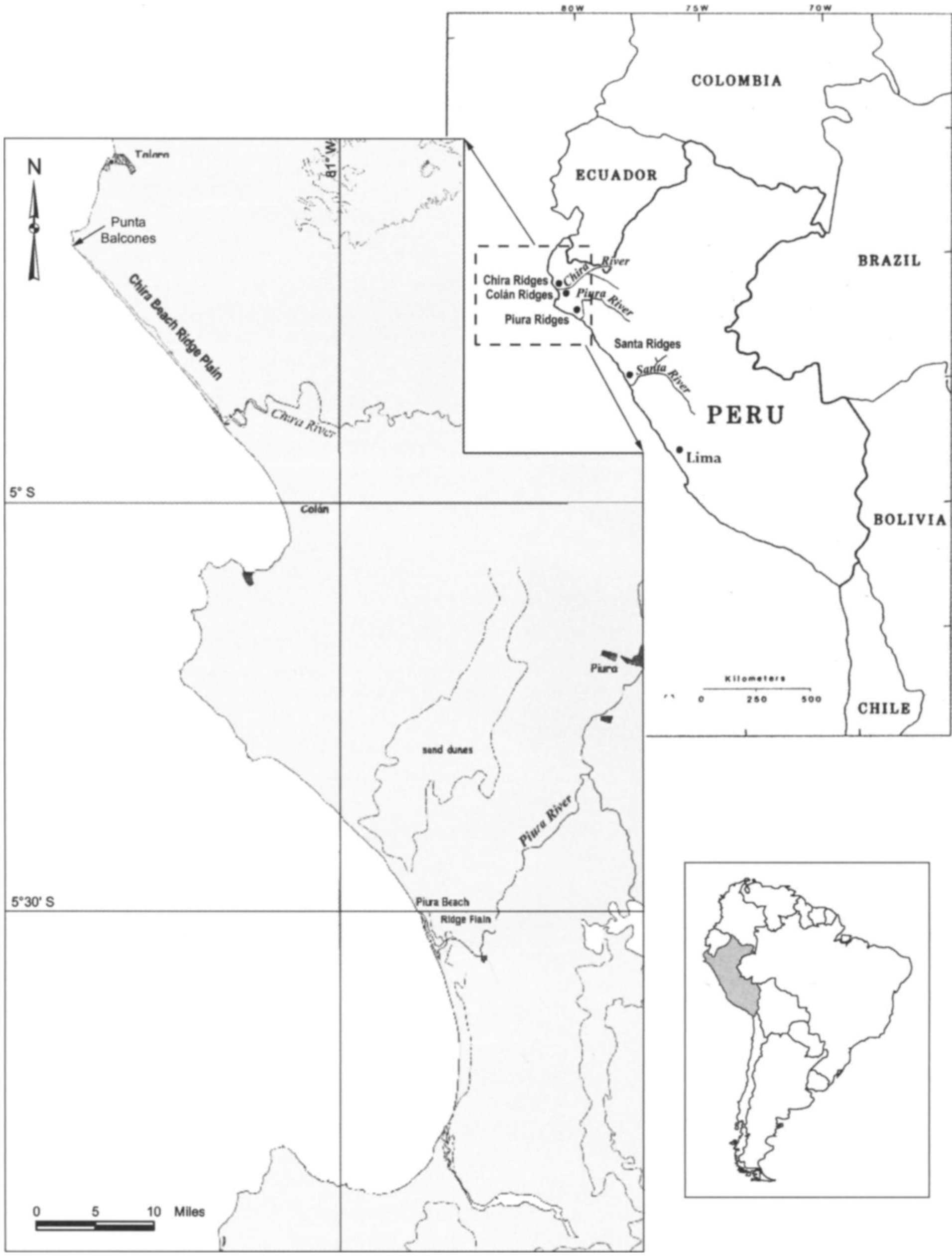

Figure 1. Map of study area showing the location of beach ridge sets and rivers.

Relict beaches are of particular interest to archaeologists because any prehistoric people who exploited marine resources would have done so from the active contemporary (now preserved) beach faces (*e.g.,* RICHARDSON, 1983; MASON, 1993).

In northwest Peru, El Niño flooding is the only known process capable of supplying large pulses of sediment to the littoral regime. When normal climatic conditions return, rapid seaward progradation occurs as longshore currents transport and redistribute the sediment northward into ridge features (SANDWEISS, 1986). In this study, we used historic aerial photographs and image processing techniques to examine the link between coastal change and El Niño activity. Differences in the shoreline position during the available period of aerial coverage (1946–1983) were measured in area to quantify actual patterns of coastal processes along the Chira, Colán, and Piura beach-ridge sets. Although no new ridge was identified at any of the locations, erosion and accretion patterns were observed and quantified at different stages preceding and following El Niño events of varying magnitude (SHAFER, 1999). Coastal processes responsible for building prehistoric beach ridges had to be inferred from sediment distribution patterns observed from the aerial photographs. This was particularly

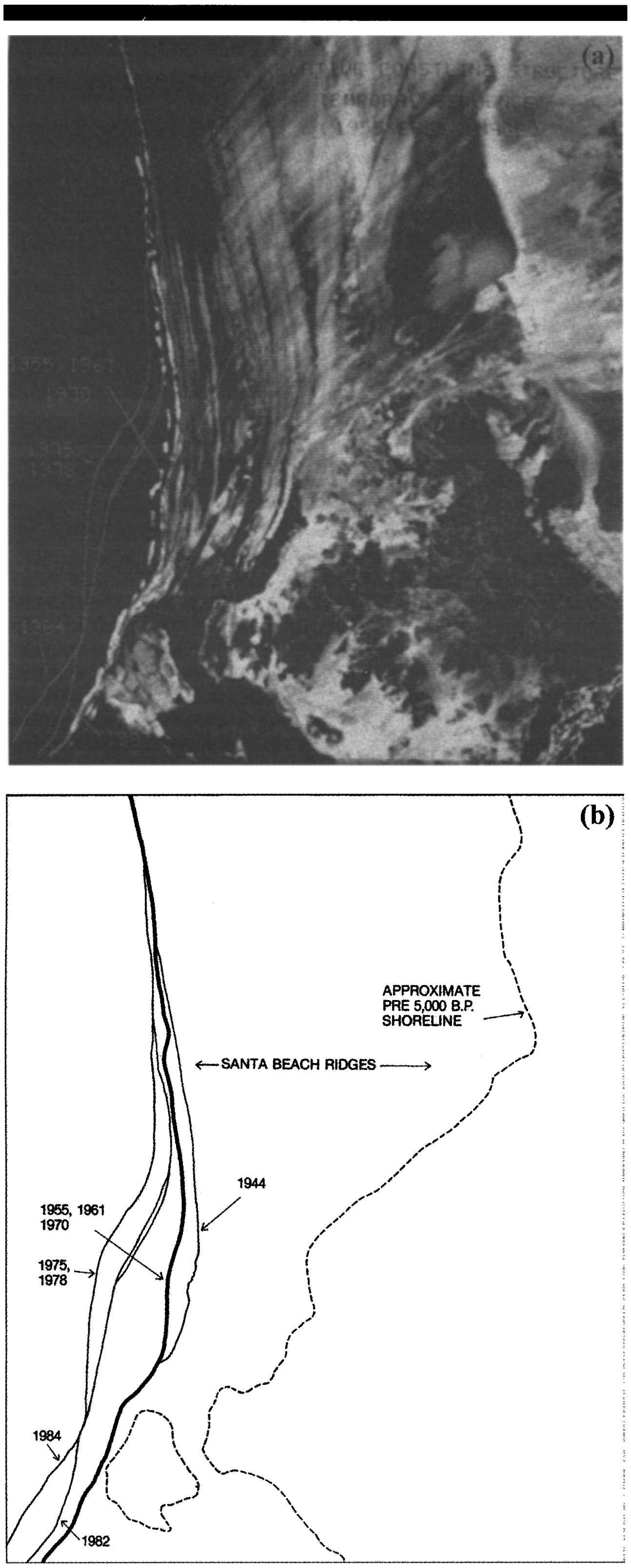

Figure 2. Results from the Santa Image Study. (a) Shoreline vectors overlaid on satellite image. (b) Line drawing of coastal changes from 1944–1984. (Reproduced from: MOSELEY *et al.,* 1992).

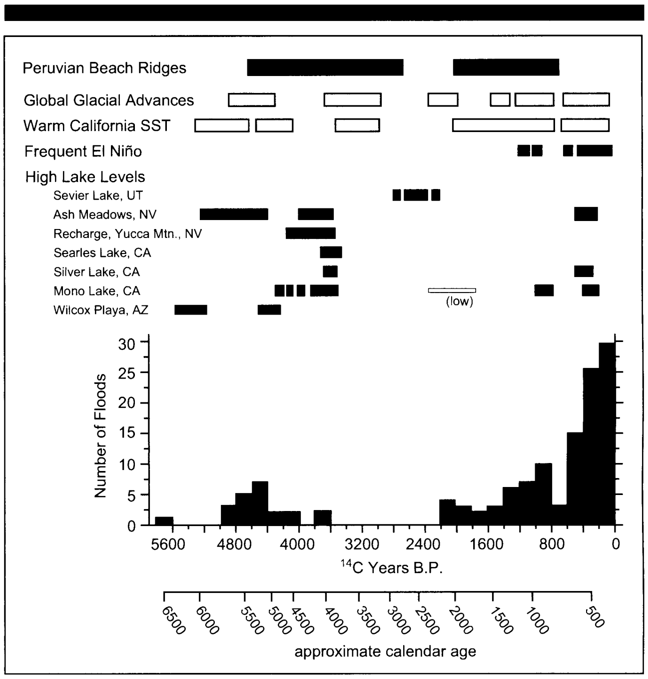

Figure 3. Paleoflood chronology for the southwestern United States compared with regional and global-scale paleoclimatic data. (Modified from: ELY, 1997). Note that the calendar year scale is non-linear as compared to the ^{14}C scale presented here.

true when establishing the potential role of El Niño in the modern coastal morphology.

Because major El Niño events likely build Peruvian ridges, beach-ridge ages may represent past, extreme El Niño events (SANDWEISS, 1986; SANDWEISS *et al.,* 1983; ORTLIEB *et al.,* 1993; WOODMAN and MABRES, 1993). Preserved ridge sets could represent mega-Niños (extraordinarily strong El Niños), which discharge proportionally large amounts of sediment (WOODMAN and MABRES, 1993). Alternatively, each ridge may be a composite built by two or more El Niño events following destabilization of the local hydrology by tectonic movement (SANDWEISS, 1986; MOSELEY *et al.,* 1992). The amount of available material is potentially enhanced by tectonic events, which release sediment into river valleys through landslides. SANDWEISS *et al.* (1983) originally introduced this ridge-formation hypothesis incorporating tectonic activity to explain the ridge set directly north of the Santa River. Alternate interpretations of beach-ridge formation mechanisms in Peru rely on sequential tectonic uplift, progradation during relative sea-level change, and glacial meltwater pulses (WELLS, 1996). Wells (1996) has also suggested that the sediment supplied during peak El Niño years is redistributed long after the occurrence of a single event.

The Santa ridges in central Peru, at approximately 9°S, have been studied in greatest detail (*e.g.,* SANDWEISS, 1986; WELLS, 1988, 1996; MOSELEY, *et al.,* 1992; SANDWEISS *et al.,* 1998). These gravel ridges indicate high energy, nearshore action during at least the last 5200 years (ORTLIEB and MACHARÉ, 1993). They are thought to form in response to strong El Niño events following intense tectonic activity (SAND-

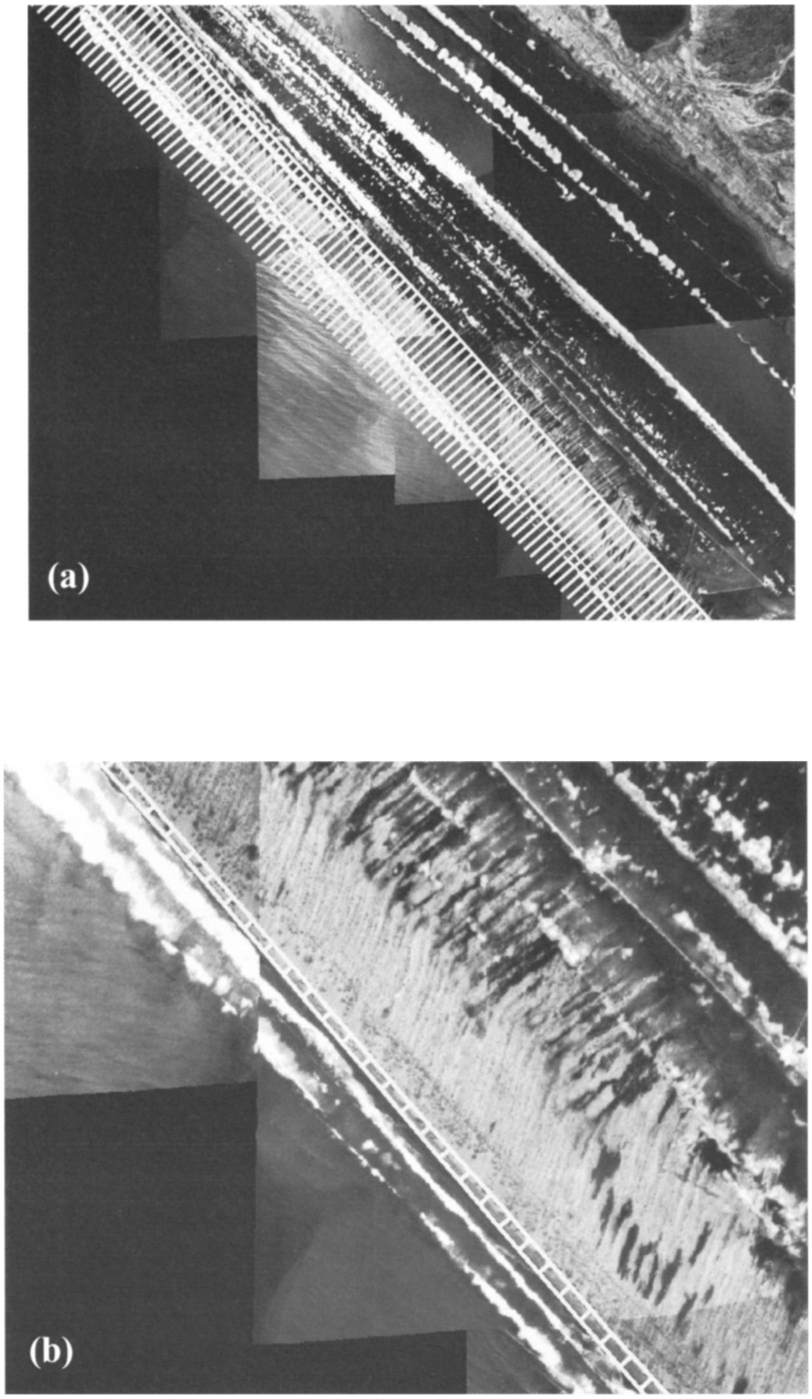

Figure 4. Methods for calculating area. (a) Perpendicular lines projected from base line across modern coastline. (b) Polygons used to calculate change along the beach ridge plains.

WEISS *et al.,* 1983; SANDWEISS, 1986; MOSELEY *et al.,* 1992).

MOSELEY *et al.* (1992) tested the seismic-El Niño hypothesis of ridge-building events by using aerial photographs and satellite imagery to identify new ridges along the Santa ridge set (Figure 2). Their work supports a combination of El Niño and seismic activity: no new beach ridge was found after the 1982–1983 El Niño event, the strongest event this century at the time of the study. However, a new ridge-like feature was identified following the 1972–1973 El Niño at the Santa beach-ridge plain. The 1972–1973 El Niño was preceded in 1970 by the strongest earthquake in the region in over half a century, which registered 7.7 on the Richter scale (PLAFKER

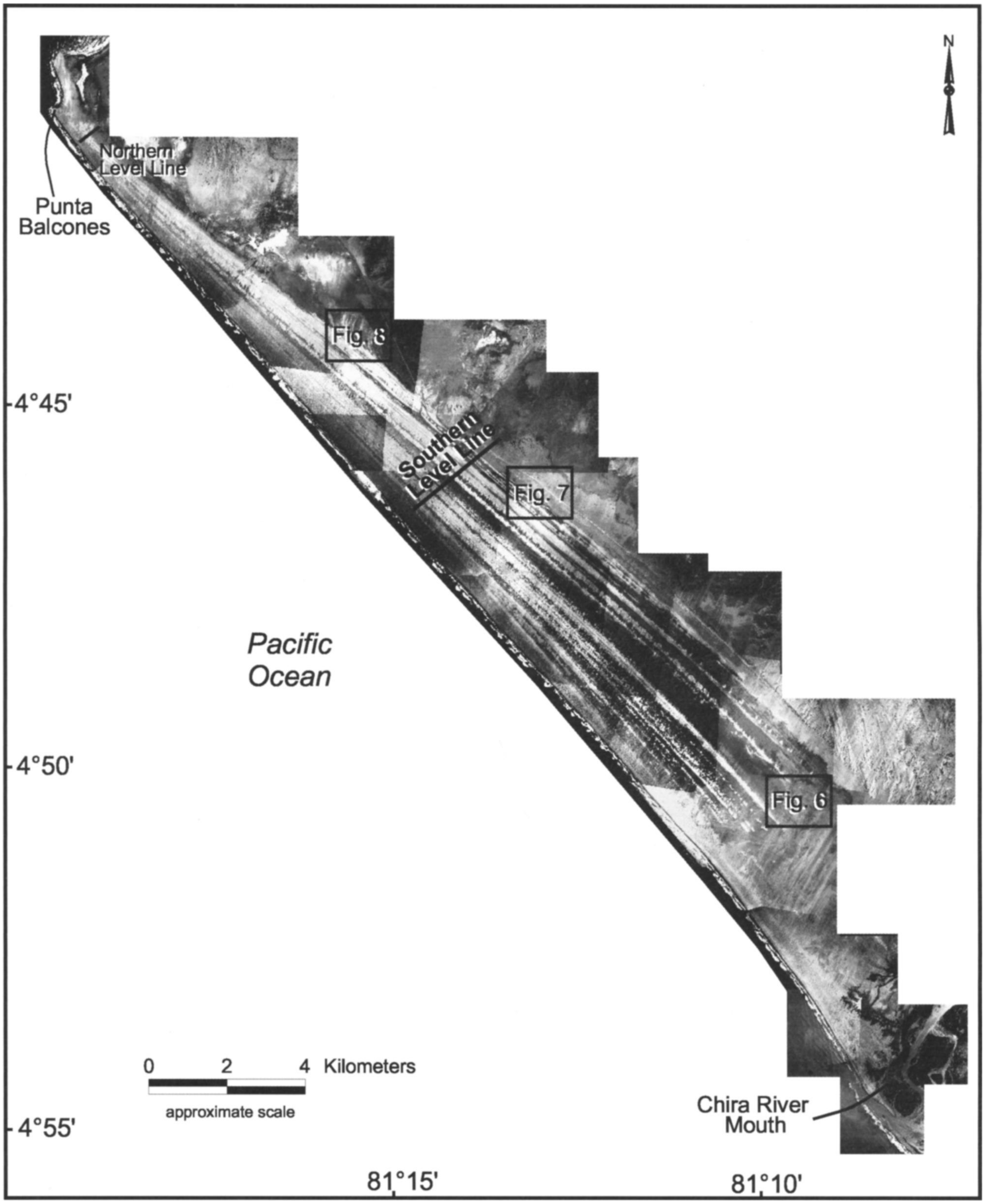

Figure 5. Photomosaic of Chira Beach Ridge Plain (1946) showing the locations of features mentioned in text.

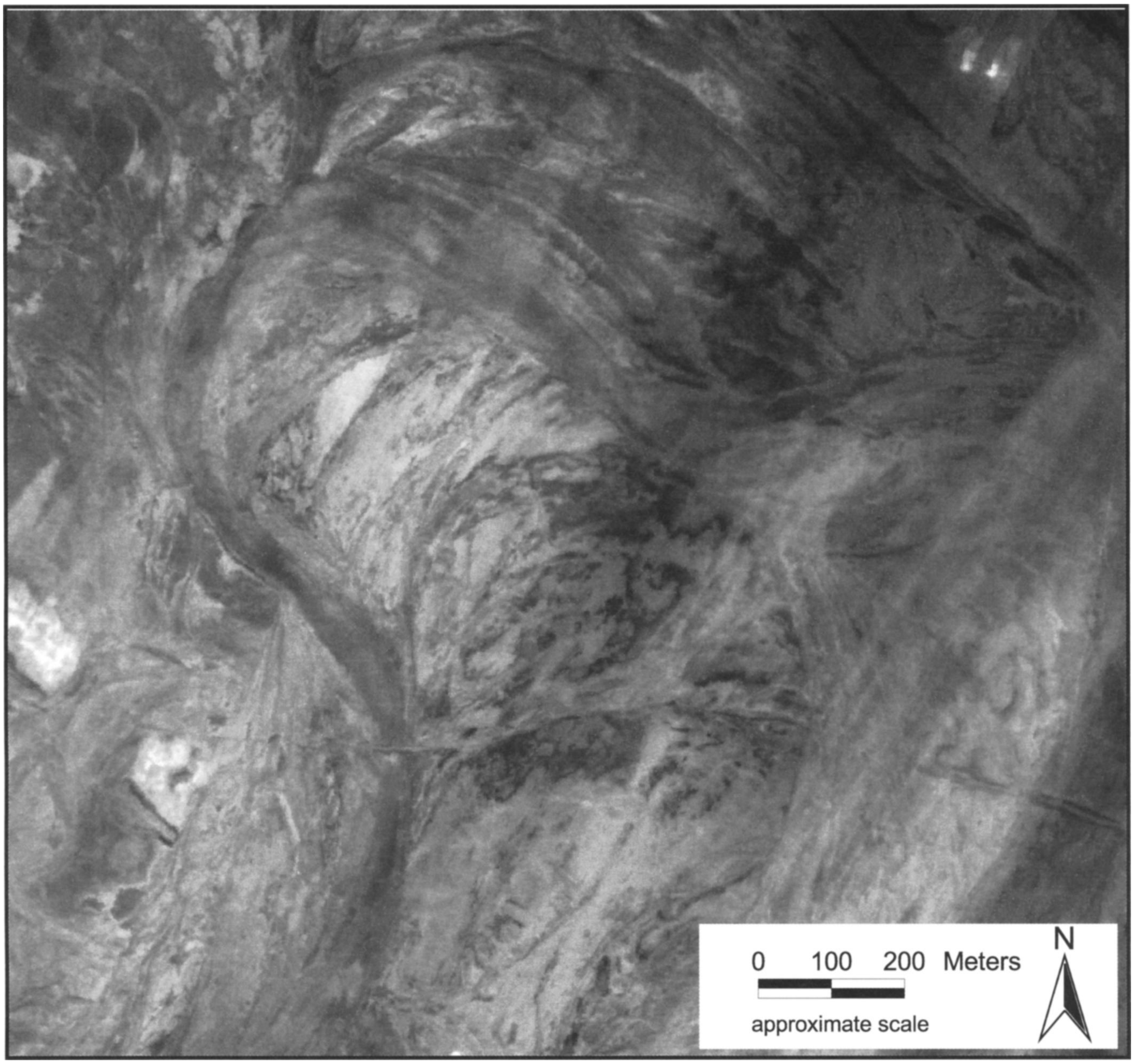

Figure 6. Scroll bars from previous river inlets at the southern end of the Chira ridges.

and ERICKSEN, 1978). These data indicate that ridges cannot provide a complete record of El Niño events, but appear to mark some extreme events that released huge amounts of sediment to the Peruvian coastlines (SANDWEISS *et al.*, 1998).

To test further the hypothesis of El Niño and seismic activity, we initiated a new imaging study at other beach-ridge plains with morphology similar to the Santa plain. The image work was supplemented by a ground-truthing survey and GPS-based georeferencing in northern Peru in June, 1997. This study concentrates on three ridge sets located north of Santa, between 4–6°S and 80–81°W: Chira, Colán, and Piura, which have the same number of ridges as Santa, as well as similar dates for the onset of ridge formation (SHAFER, 1999). The Chira and Piura ridge plains were also the subject of other studies (*e.g.,* ORTLIEB *et al.,* 1993; RICHARDSON, 1983). For example, RICHARDSON (1981, 1983) focused on environmental factors affecting the emergence of maritime-based societies on the Peruvian coast. He used the ridges to ascertain the date for the establishment of modern climate and the formation of the present coastline. RICHARDSON (1983) determined that 5800 cal yrs BP, just prior to the initiation date of beach-ridge preservation, was also a date crucial to under-

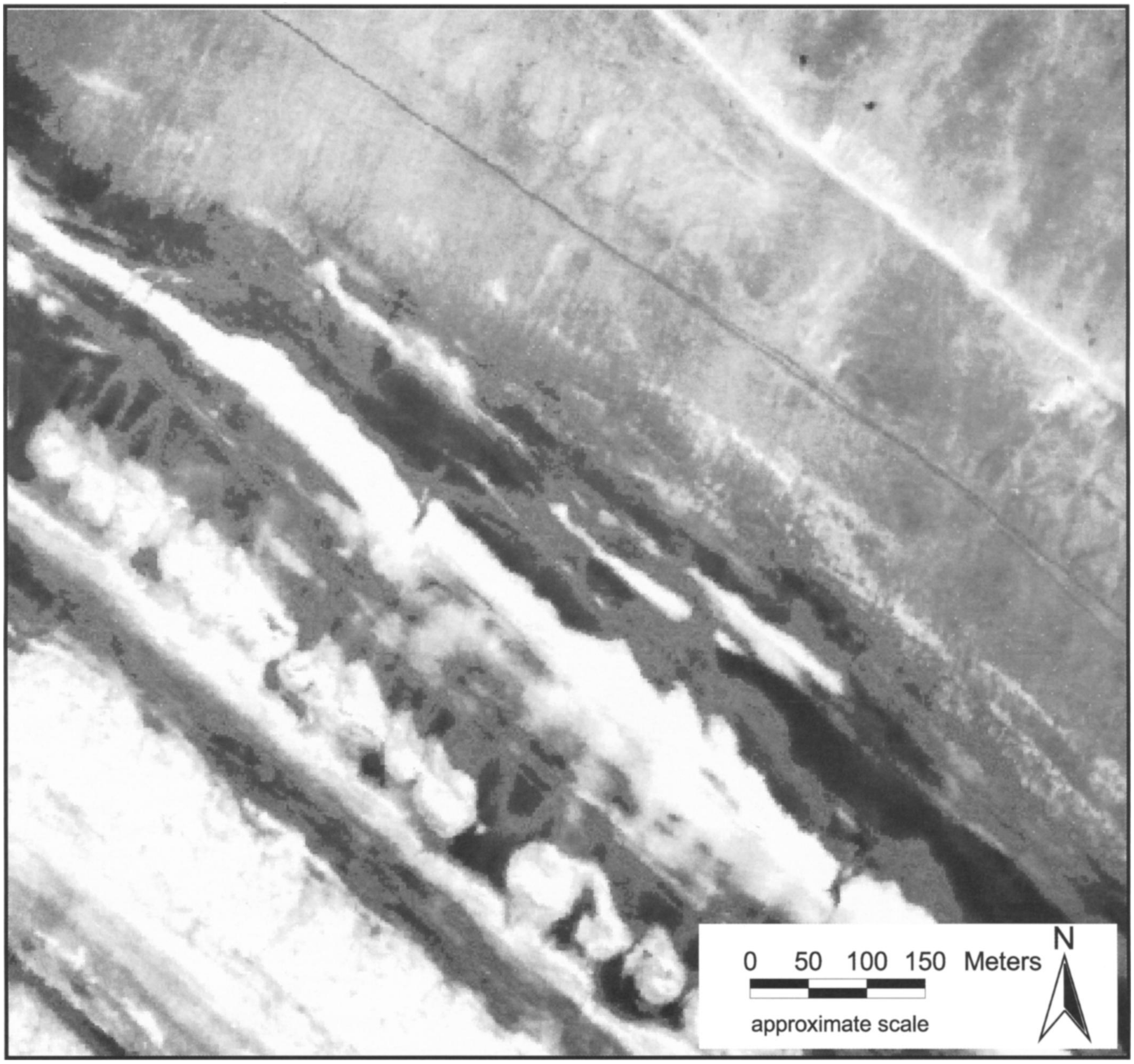

Figure 7. Oldest Chira ridge showing broken and disintegrating sections.

standing the rise of complex maritime societies in coastal Peru.

The average annual flow of the Chira River is 5500×10^6 m^3, the greatest of any river in the Coastal Desert north of the Santa River (9°S), and it brings more material to the shoreface for redistribution by the longshore current than the Piura River. The Chira River also has a longer course, and its headwaters reach the southern margin of the tropical rainfall area near Ecuador, where the annual flow is maintained by snowmelt (MEIGS, 1966). While both the Chira and Piura Rivers have headwaters in the Andean foothills, Piura lacks snowfields in its headwater area (MEIGS, 1966). In normal years the flow of the Piura River did not reach the coast, until it was supplemented for agricultural purposes in 1953 by Rio Quiroz (BOSWORTH, 1922; MEIGS, 1966). The Piura ridges extend approximately 10 km from south to north, in comparison with the 30-km long Chira ridge plain; the shorter length of the Piura ridges may be due in part to the lower river volume, to the geometry of the coastal compartment, and to differences in potential sediment supply. Colán differs from the other three ridge sets discussed here, because there is no river feeding material to the beach ridges. Instead, the

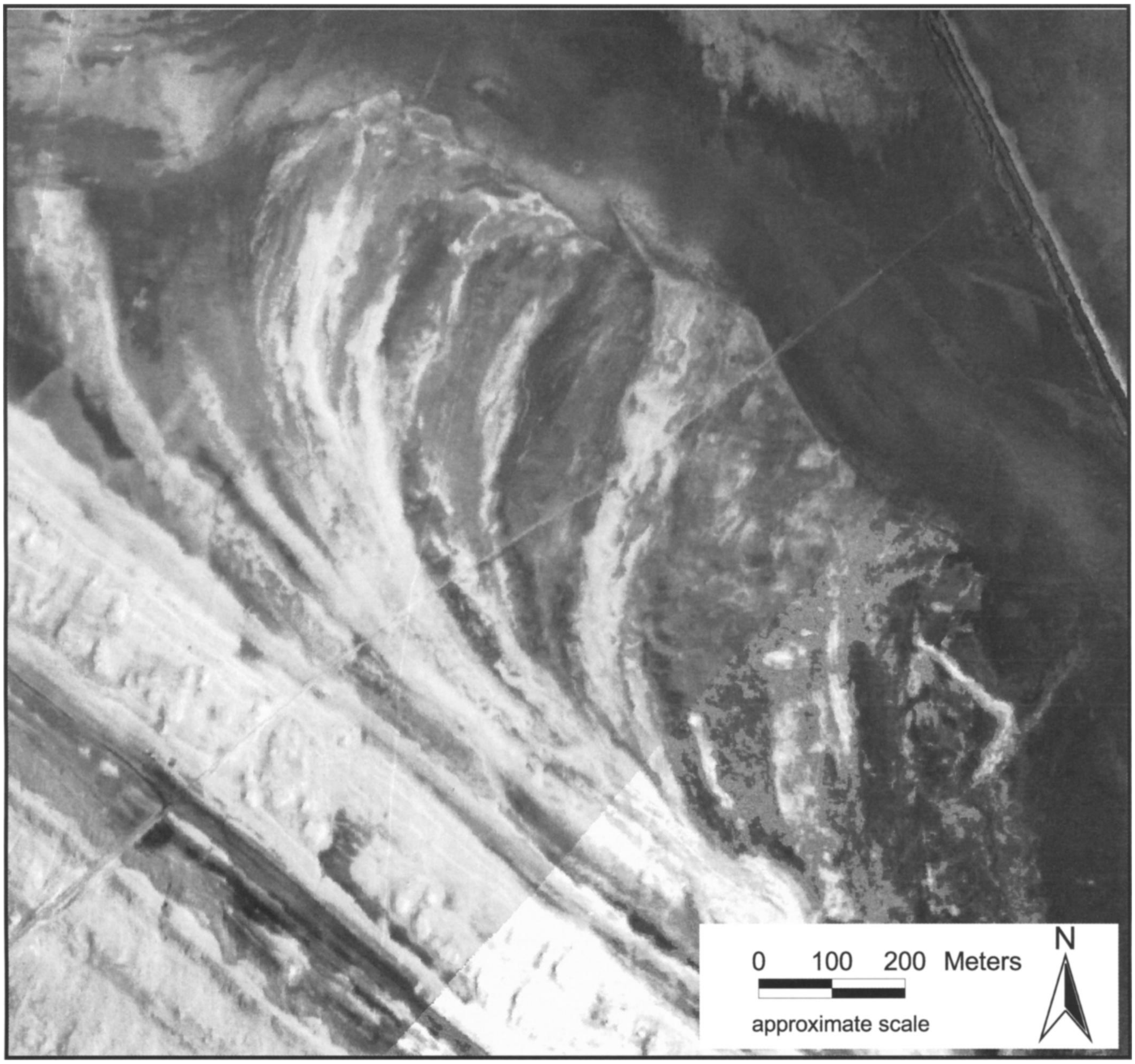

Figure 8. Recurved spits behind the Chira ridge plain.

gravel comes from a Quaternary conglomerate and sandstone sea cliff, which flanks the coastal plain.

Only eight to nine ridges have formed at each of the plains since ca. 5200 cal yrs BP, the minimum date for the first, farthest landward ridge, similar to the Santa area ridges. The oldest two to four ridges at both Colán and Chira formed between 5180 and 2,500 cal yrs BP (ORTLIEB *et al.,* 1993). The other five ridges, closer to the shoreline, were dated younger than 2,500 cal yrs BP (ORTLIEB *et al.,* 1993). The sand morphology of both the Chira and Piura ridge sets contrasts with the coarse gravel ridges at Colán and Santa. In each ridge plain, each succeeding ridge dates to a progressively younger time period in a seaward direction, and a new ridge was preserved on average every 500 years (SANDWEISS, 1986; ORTLIEB *et al.,* 1993; RICHARDSON, 1983). This may mean that not every ridge created was preserved, or that a single ridge was built approximately every 500 years. During the period studied by aerial photo analysis, 1946–1983, El Niños occurred on average every four years (SHAFER, 1999). Between 1946 and 1955 two El Niño events occurred, both rated moderate (M) in strength (QUINN *et al.,* 1987). From 1955 to 1983, seven El Niños occurred, all either moderate or

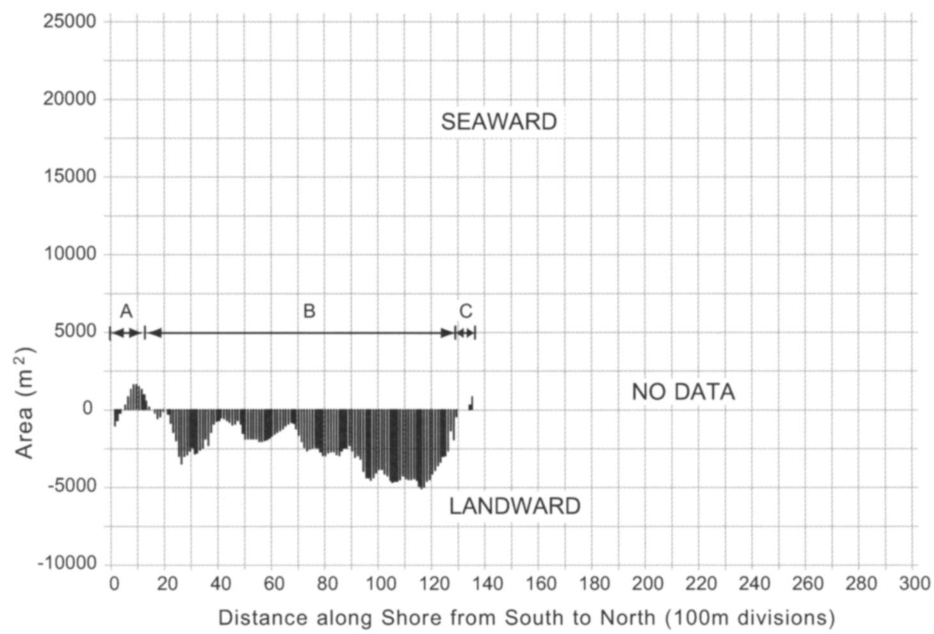

Values for Chira 1946-1948 (x 1000 m^2)

A	B	C	Std Dev	Median	Average	Minimum	Maximum	Total Erosion	Total Accretion
7.8	-291.8	1.0	1.6	-2.1	-2.1	-5.1	1.6	-294.0	11.0

Figure 9. Chira shoreline change measurements, 1946–1948.

strong (QUINN *et al.,* 1987). The 1972–1973 El Niño was rated strong (S) and the 1982–1983 El Niño was rated very strong (VS). Examination of the available imagery and timing of historic ENSO events offers further insight into ridge-forming processes at the northern ridge sets, and the potential uses of beach ridges as a paleoclimatic indicator of El Niño.

Holocene El Niño Variability

Proxy records used to reconstruct paleo-El Niño chronologies include flood deposits, laminated sediments, lake-level fluctuations, ice cores, sediment cores, and faunal associations (ORTLIEB and MACHARÉ, 1993). Several paleoclimatic indicators suggest that the El Niño phenomenon, as it is presently understood and experienced in the modern Peruvian coastal environment, did not occur during the early Middle Holocene (SANDWEISS *et al.,* 1996, 2001). Multiple sources of evidence, including pollen data, lake records, corals, geomorphology, and geoarchaeology, support the hypothesis that ENSO was absent or extremely rare between ca. 9000 and 5800 cal yrs BP (*e.g.,* ELY *et al.,* 1993; LEES, 1992; SHULMEISTER and LEES, 1995; MCGLONE *et al.,* 1992; TUDHOPE *et al.,* 2001; ANDRUS *et al.,* 2002). SANDWEISS *et al.* (2001) provide evidence from archaeological mollusks and other paleoclimatic proxies that from ca. 5800 to 3000 cal yrs BP, El Niño was present but less frequent than today; the modern range of recurrence intervals for ENSO apparently started only after that time.

Brazilian beach ridges may also show a change in the frequency of El Niño, though the timing is different from that proposed by SANDWEISS *et al.* (2001). MARTIN *et al.* (1993) suggest that El Niño-like conditions occurred before 4320 cal yrs BP, but were absent during 4320–3900 cal yrs BP and 2880–2580 cal yrs BP After 2580 cal yrs BP El Niño became active again, but more infrequent. Beach ridges in Brazil would not have been built or preserved when El Niño was absent. Periods when no new ridges formed occurred during episodes of sea-level fluctuations, specifically submergence, but beach ridges did form during periods of emergence. Thus, if El Niño were still occurring during periods of submergence (4320–3900 cal yrs BP and 2880–2580 cal yrs BP), the record would have been obscured, if not completely erased by the regionally higher sea levels.

Further support for a period of less active ENSO events comes from the southwestern United States. Floods are anomalous in the normally arid to semiarid environment of the southwest United States (ELY *et al.,* 1994). Paleoflood data from 19 rivers in Arizona and Utah revealed clusters of activity over the last 6000 years, which were most numerous between 5800–3900 cal yrs BP, 980–880 cal yrs BP and after 520 cal yrs BP (Figure 3) (ELY, 1997; ELY *et al.,* 1993, 1994). A marked decrease was found between 3900 and 2250 cal yrs BP, as well as a short but distinct decrease from 800 to 600 yrs BP (ELY, 1997; ELY *et al.,* 1993, 1994). The 3900–2250 cal yrs BP episode agrees with the findings of MARTIN *et al.*

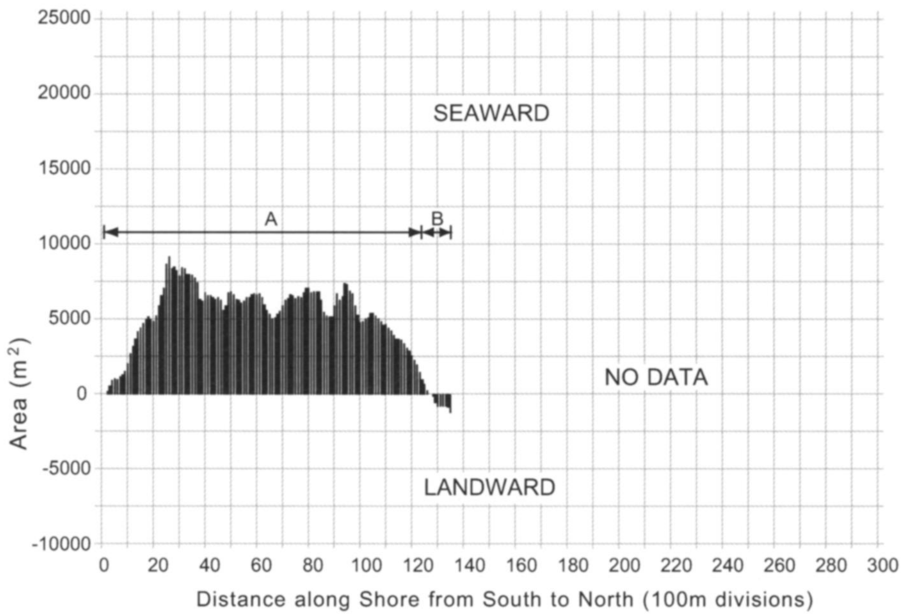

Values for Chira 1948-1955 (x 1000 m^2)

A	B	Std Dev	Median	Average	Minimum	Maximum	Total Erosion	Total Accretion
6,737.2	-5.8	2.5	6.6	5.0	-1.2	9.1	-5.8	6,737.2

Figure 10. Chira shoreline change measurements, 1948–1955.

(1993), and coincides with drier conditions determined from lake sediments. The paleoflood chronology from the Casma River (WELLS, 1987, 1988, 1990) indicated one large flood approximately dated at 3400 cal yrs BP, and another between 3220–2580 cal yrs BP The deposits include material that was radiocarbon-dated; however, these data come from only one river valley unlike the multiple-river-valley paleoflood stratigraphy of the southwest U.S.

METHODS

This study consists primarily of aerial photo analysis, supplemented by groundtruthing during the summer of 1997. At that time, we gathered differentially corrected GPS coordinates for photo-identifiable locations along the Chira ridges and uncorrected GPS coordinates at the Colán and Piura ridge plains. In the field we also studied the geomorphic and sedimentary characteristics of the Chira, Colán, Piura, and Santa beach-ridge plains.

Imagery Sources·

Vertical black and white aerial photographs were used to assess changes in the Northern Peruvian beach-ridge sets over a recent 37-year time period. Change detection is the process of identifying differences in the state of an object or phenomenon by observing it at different times in the past. The extent of change can then be measured and spatial patterns assessed (MACLEOD and CONGALTON, 1998). Paper copies of the Peruvian aerial photos were obtained from Peru's Servicio Aerofotográfico Nacional. The available coverage years for Chira were 1946, 1948, 1955, and 1983; the photos varied in scale from 1:20,000 to 1:70,000. Piura aerial coverage was available from 1946, 1955, 1965, 1970, and 1972, at scales varying from 1:6000 to 1:70,000. A single set of 1946 photographs was available for Colán, thus change detection was not possible at that location.

The nature of change detection makes quantitative estimates of accuracy difficult due to problems of obtaining reference data for images taken in the past. Errors tend to propagate throughout change-detection due to the large number of variables associated with the process, such as radiometric differences and registration issues between photo sets (MACLEOD and CONGALTON, 1998). Geometric distortion within aerial photographs originates from topography, lens distortion, and film deformation (THIELER and DANFORTH, 1994). Further error is introduced in the development of negatives and generation of prints. The photographs used in this study could not be orthorectified to standardize sources of inconsistency due to the lack of digital elevation models (DEM) and an adequate camera information report. Because the coastal plains in the study areas were all relatively flat, abrupt elevation change was not an issue for accurate analysis. The photos were all gathered using the same method; therefore

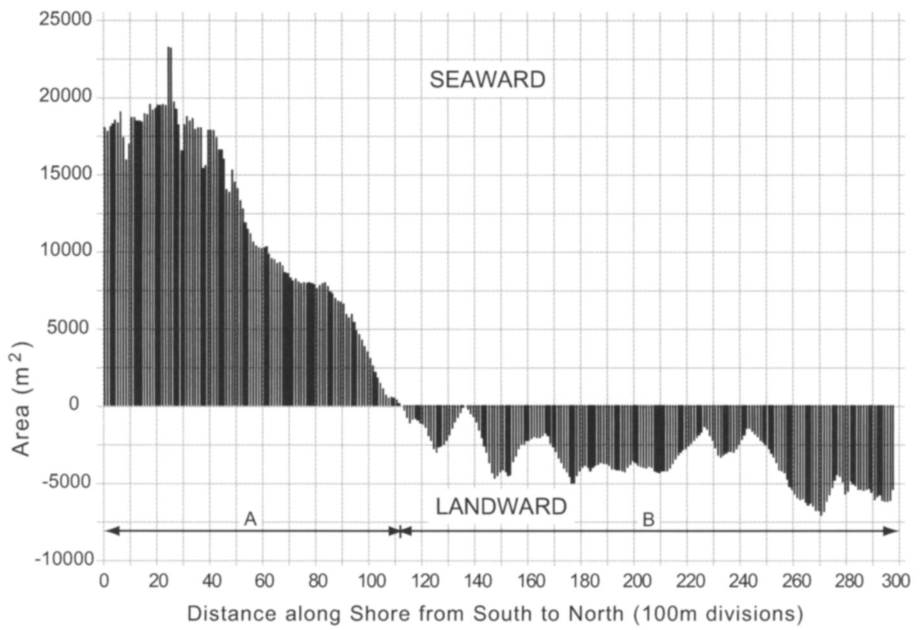

Values for Chira 1946-1983 (x 1000 m^2)

A	B	Std Dev	Median	Average	Minimum	Maximum	Total Erosion	Total Accretion
1,330.9	-651.9	8.5	-2.0	2.3	-7.1	23.2	-651.9	1,330.9

Figure 11. Chira shoreline change measurements, 1946–1983.

comparisons could be made more reliably and accurately than integrating several different types of imagery.

Change Detection Methods

Analysis of large areas using aerial photographs requires the creation of an image mosaic composed of multiple aerial photographs. The aerial photographs for each beach ridge plain were scanned and a mosaic of each time period was created, which combined up to 30 photo frames into one image. The aerial photographs of the Peruvian beach-ridge sets were scanned from the available prints, and the scanning resolution was adjusted based on the photo-scale such that the output digital image resolution was 2 m/pixel. Only the middle portion of each photograph was used in order to minimize distortion encountered on the edges of the photographs, farther from the focal region. Control points between consecutive pictures within a region of overlap were used to "rubber-sheet" one of the photos to a control image using the finite element, Delauney Triangulation, resampling method. Accurate geographic registration between consecutive images can be difficult in remote regions, where there are few stationary identifiable points between photo sets of different years (Thieler and Danforth, 1994). Aerial photograph mosaics were created based on common features that remained constant over time between consecutive pictures using *Intergraph's MGE Base Imager.* The beach ridge mosaics were georeferenced with GPS coordinates gathered in the field for some common features after the photos were assembled into a single image.

Prior to change detection the imagery must be geometrically rectified such that identical pixels overlap the same geographic location on all dates of coverage (Macleod and Congalton, 1998; Crowell *et al.,* 1991). To orient each mosaic correctly to the real-world location of features, one photomosaic for each region was resampled to match a chart or satellite image and acted as a control for the other time periods. Each subsequent mosaic representing the same region at different time periods was spatially rectified to match the control image. Once the mosaics were correctly oriented they were brought into *ERDAS Imagine 8.3* and georeferenced using Global Positioning System (GPS) field data gathered during June, 1997. Each subsequent year for a given region was resampled to match the original georeferenced mosaic, to ensure that any change measured on the images accurately reflected changes on the ground. This process standardized errors among image sets of different years. Although the actual mosaics may still contain some geometric distortions, the different photomosaics within each region have consistent errors, allowing for reliable relative measurements of change.

Shoreline Identification

Different coastal environments lend themselves to several types of control lines, such as the line of vegetation, the dune

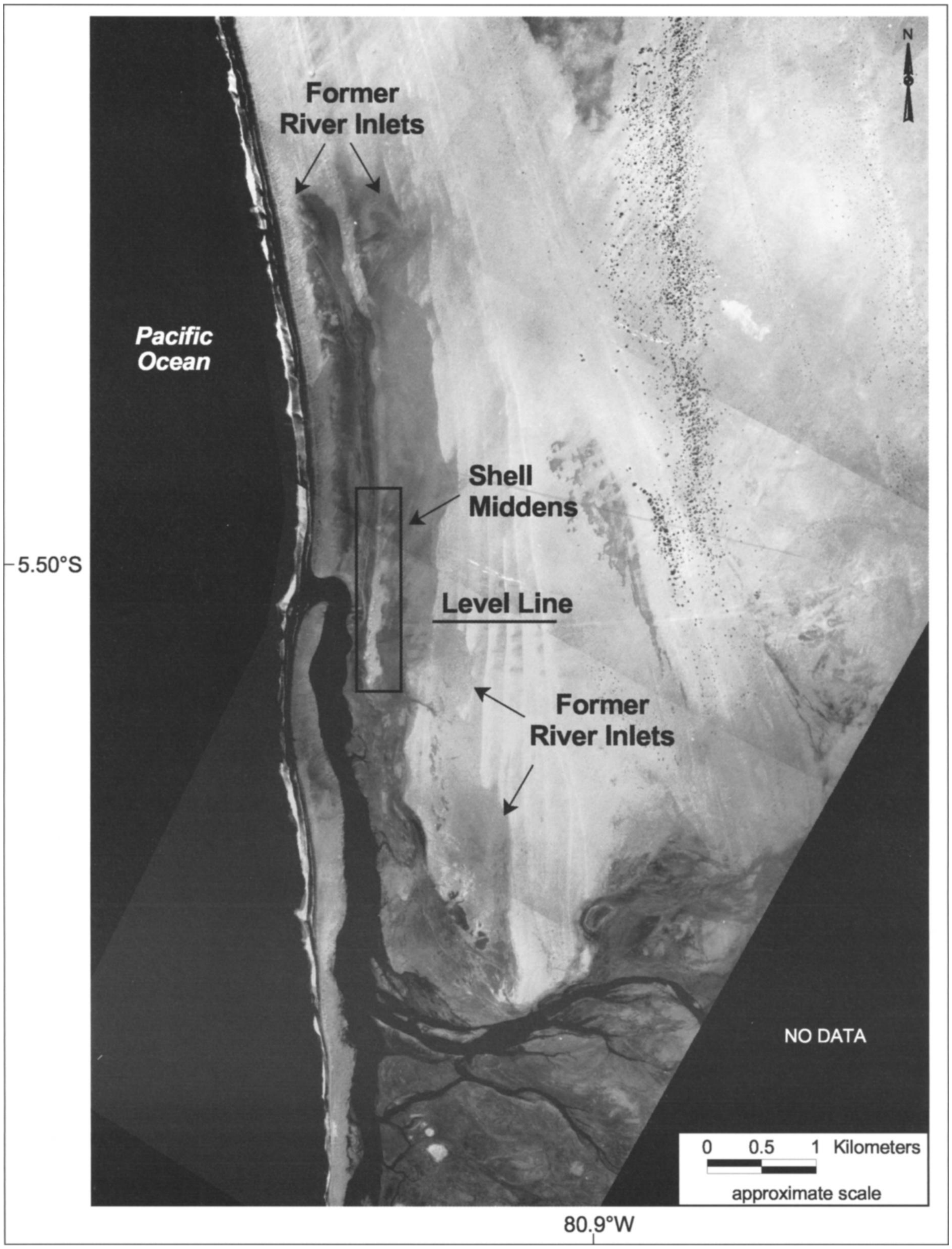

Figure 12. Photomosaic of Piura River and Beach Ridge Plain (1946).

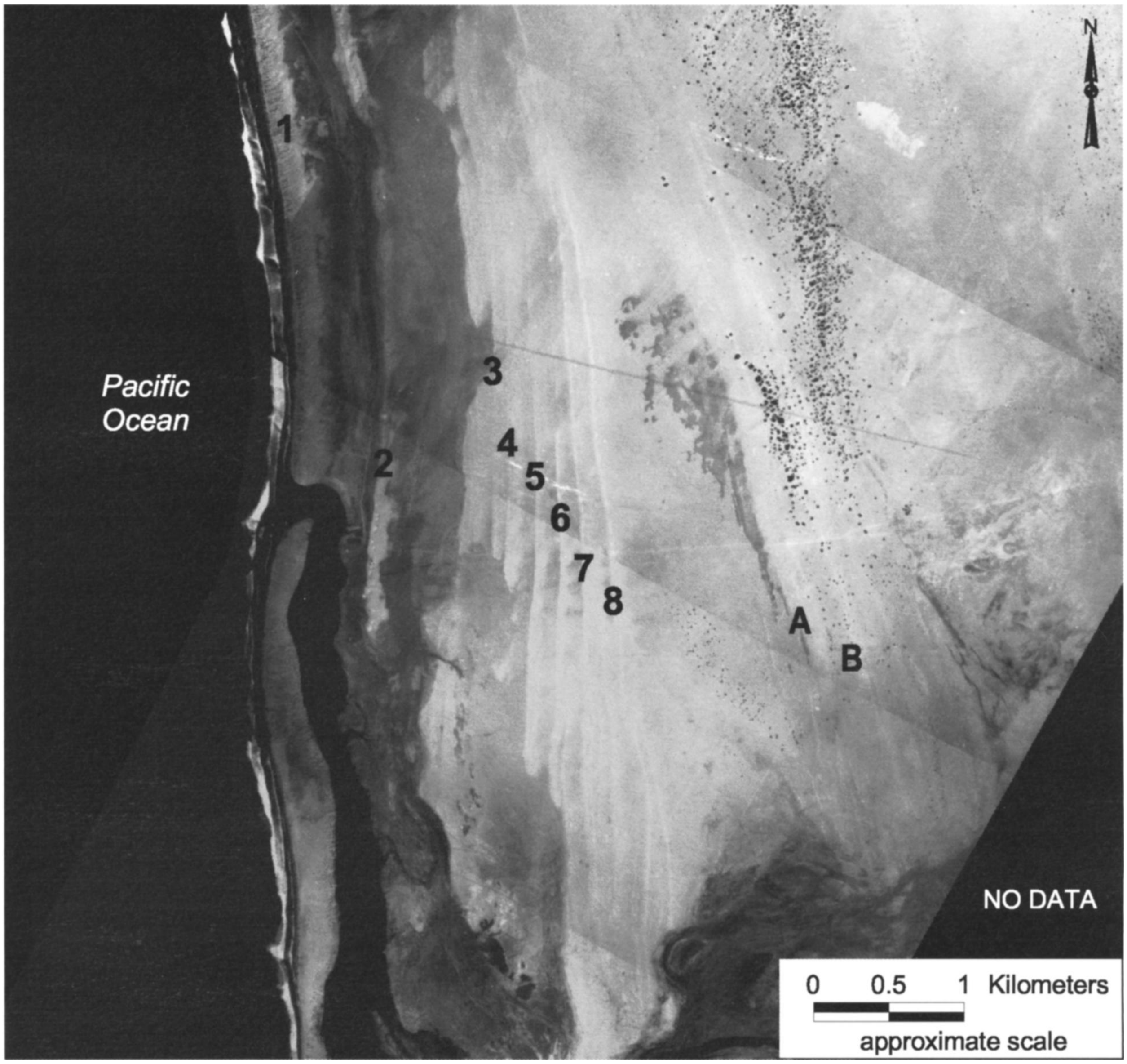

Figure 13. Number scheme of the Piura ridges. Letters A–B show the location of additional landward ridges that were not included in the earlier numbering scheme (RICHARDSON and MCCONAUGHY, 1987).

foot, or the high water line (JIMENEZ *et al.,* 1997; THIELER and DANFORTH, 1994). The water/land interface was chosen for comparison in this study because the Peruvian coast is a microtidal environment. The microtidal range of 0–2 m does not significantly change the water/land location throughout the course of a daily or monthly tidal cycle. In contrast, the dune or vegetation line along the Peruvian coastlines in the study areas was too irregular to make consistent comparison measurements. In the northern section of the Chira ridges there is a distinct erosional scarp, however in the southern area the dunes do not form linearly parallel to the coastline. Furthermore, during El Niño years sea level can rise by up to 60 cm, thus the use of a high-tide or wet/dry line along the shoreface would have been impossible on the 1972 and 1983 photo sets.

Throughout the photo sets there were significant contrast variations depending on the light angle in the water and the shoreline, making edge extraction attempts unsuccessful. Although these discrepancies could be recognized and compensated for by an analyst, the computer could not be relied upon to differentiate the water/land interface accurately under different light angles and intensities. Thus, the shoreline was digitized by hand onscreen in *ERDAS Imagine 8.3* from the large photomosaics. The arcs were saved as *Arc/Info* coverages for further analysis within *Arc/Info 7.2.1* and *ArcView 3.0a* GIS software.

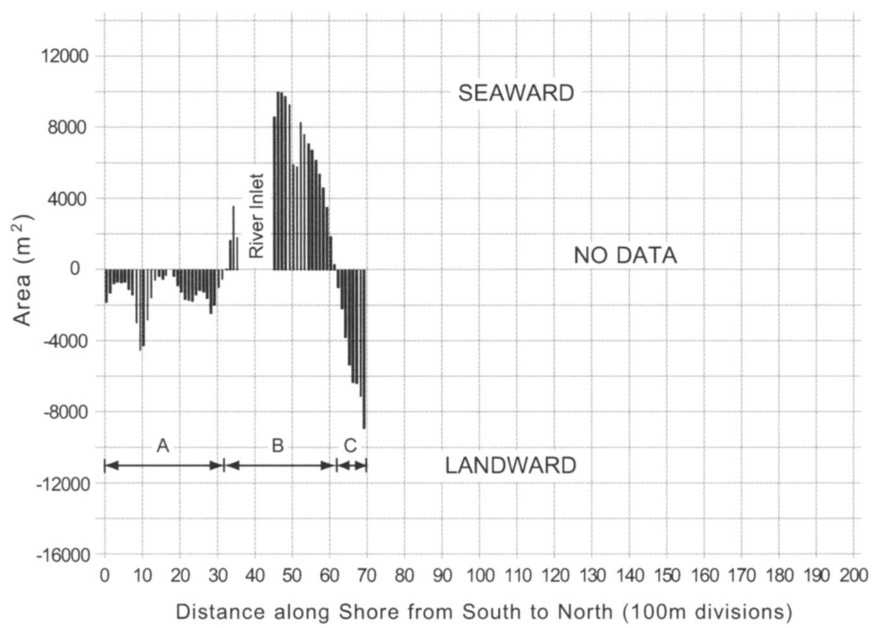

Values for Piura1955-1965 (x 1000 m²)

A	B	C	Std Dev	Median	Average	Minimum	Maximum	Total Erosion	Total Accretion
-45.8	117.5	-4.1	4.5	-0.7	0.5	-8.9	10.0	-86.9	117.5

Figure 14. Piura shoreline change measurements, 1955–1965.

In *Arc/Info* the shoreline arcs from Chira and Piura were divided into 100 m segments along a baseline, and change over time was quantified in area. The base line was created from the first year of available data, which for both Chira and Piura was 1946. The 1946 digitized shoreline was copied and moved landward by 500 m to create a parallel control line. The control line was broken into a series of shorter lines, each 100 m long (Figure 4). Using *Arc/Info Macro Language* (AML) a program was written to calculate the perpendicular to each of these shorter arcs. Points were projected seaward by 1 km along the perpendicular line. The *Arc/Info* command *GENERATE* was used to create lines between the break point in the control line and its corresponding projected point. The perpendicular lines were intersected with combinations of shorelines from different years to create polygon files (Figure 4). Then the polygons were manually coded as either erosional or accretional based on the relative location of shoreline arcs from different years, and the area was measured in square meters.

We supplemented the area measurements with observations of coastal change made through visual comparisons of the photomosaics among the years of aerial coverage. In addition, modern coastal behavior was deduced from evidence of past processes preserved in the beach-ridge plains, assuming that the coastal processes remained consistent over the past 5200 years. The measurable error (precision) is 2 m of variability throughout the image results for all three beach-ridge plains based on the scanner resolution and photo scale. For Chira, the only beach-ridge set for which differentially corrected GPS data could be gathered, the accuracy of the georeferencing is 3–5 m. Each year of aerial photo coverage was measured against the next in temporal order, and the earliest year of coverage was compared to the most recent. For example, in the Chira dataset, 1946 was compared to 1948, then 1948 to 1955 and 1955 to 1983, and total change was measured between 1946 and 1983 in the final dataset.

RESULTS AND DISCUSSION

Chira Image Mosaics

The four oldest continuous ridges along the Chira plain are separated from the younger, more seaward ridges by a large swale that extends the entire 30-km length of the ridges (Figure 5). There are no complete ridges remaining near the Chira River mouth due to past river-mouth migration. Only scroll bars and small segments of remnant beach ridges remain (Figure 6). The oldest ridge, which is farthest inland, is broken in many places (Figure 7). At its northernmost point the oldest ridge becomes a series of low-lying recurved spits (Figure 8). The spits are composed of quartz sand and carbonate shell hash, which was reworked into smaller fragments and deposited within sandy structures by repetitive wave action. The existence of recurved spits implies that at higher sea levels, such as during paleo-El Niño events, the

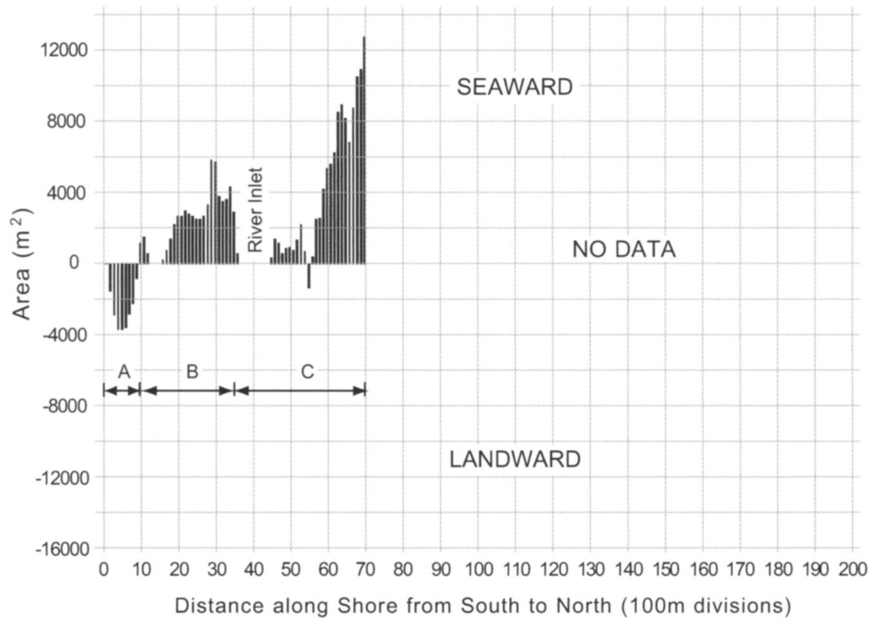

Values for Piura1965-1970 (x 1000 m^2)

A	B	C	Std Dev	Median	Average	Minimum	Maximum	Total Erosion	Total Accretion
-21.4	62.4	12.7	3.6	2.2	2.4	-3.7	12.7	-22.8	174.4

Figure 15. Piura shoreline change measurements, 1965–1970.

oldest ridge at Chira was either a barrier with an inlet or a terminal spit prograding into a lagoon. All subsequent, younger ridges extend the entire length of the plain from directly north of the Chira River to immediately south of Punta Balcones, a Cretaceous bedrock outcrop. Punta Balcones provides a topographic constraint to ridge growth and helped the Chira ridges to coalesce into a wedge-shaped deposit over the last 5200 years. There was more lateral accommodation space for progradation and sediment accumulation in the southern end of the ridge plain. Separating this geomorphic control from the longshore diminution in coarse sediment supply is difficult. As the plain narrows, the ridges become hummocky and the swales disappear, making it impossible to discern individual features. Two kilometers northeast of Punta Balcones is the opening for the modern day inlet, which is activated during El Niño periods when ocean and flood water pool behind the ridge plain.

The most distinctive feature of the Chira ridges is their shell cap. The shell cap measures up to 10 cm thick on older ridges. However, the variability of the cap thickness along and across the ridges has not been evaluated. The top shell layers are convex up, due to wind action, but below the surface the shells are distributed haphazardly. The accumulation of shell debris maintains the size of older sand ridges; otherwise, the ridge sand would be blown inland by strong onshore winds. Survey data gathered during the summer of 1997 measured the height of the largest Chira ridges in the southern section as 6 meters above sea level. Near the modern shoreline there are no shells on top of the modern dunes, halophylous vegetation holds the sand in place. Sand that is not captured by vegetation at the shore is blown landward and forms longitudinal dunes near the modern coastline. As sand moves progressively farther inland it joins the fields of barchan dunes. Eventually the sand migrates back into the river valleys, and travels in a cyclical manner back to the shoreline (MOSELEY *et al.,* 1992).

The shell accumulation that protects the Chira ridges, made up of the species *Donax obesulus* and *Tivela hians,* is the result of both natural and human sources (RICHARDSON, 1983). Prehistoric middens can provide a source of shell material (RICHARDSON, 1983; ORTLIEB *et al.,* 1995). The presence of prehistoric humans along the Chira ridge plain is evident in surface scatters of tools, hearths, and pottery remains. It is assumed that prehistoric shellfishers left their debris on the beachface and frontal dune ridge. As the shell material accumulated the sand base was protected from deflation and floodwaters. Any refuse heaps left by aboriginal peoples would also be reworked by strong El Niño storms and thrown up to the highest reach of the storm waves. Additionally, some shell accumulation may be the result of mass shellfish deaths caused by prehistoric El Niño activity (*e.g.,* ARNTZ, 1986). During the El Niño of 1982–83, ARNTZ (1986) noted increased mortality of *Donax* and *Tivela* on some Peruvian beaches. Abnormally strong waves, common during El

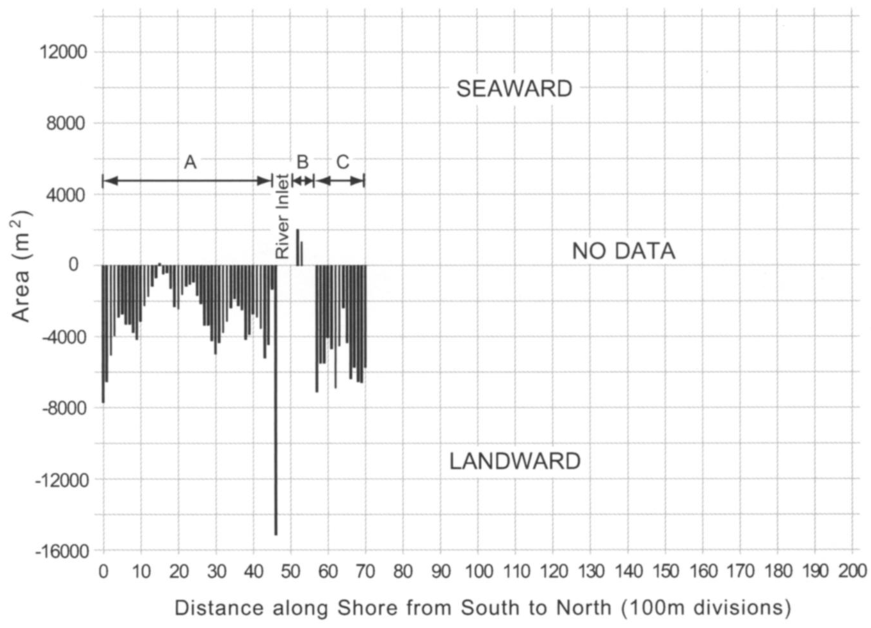

Values for Piura1970-1972 (x 1000 m²)

A	B	C	Std Dev	Median	Average	Minimum	Maximum	Total Erosion	Total Accretion
-147.4	3.3	-76.1	2.5	-3.3	-3.4	-15.8	2.0	-223.5	3.3

Figure 16. Piura shoreline change measurements, 1970–1972.

Niño, would have then stranded the dead shellfish at their farthest reach, the highest point on the beach surface.

Chira GIS Data and Analysis

The earliest historic aerial photographs of the Chira region cover a short time interval, 1946–1948. The 1948 photos were available for only the southern portion of the ridge set. The GIS results show that the period from 1946 to 1948 was dominated by erosion in the 11–12 km southern section, closest to the river mouth (Figure 9). The erosion trend noted between 1946 and 1948 contrasts greatly with the Chira data from 1948–1955 and 1955–1983, when the same location experienced extensive progradation. Between 1948 and 1955 the southerly section of the Chira ridges experienced overall accretion in the 11 km closest to the river mouth (Figure 10). Approximately 12–13 km north of the river mouth this trend switched to erosion. There were no El Niño events between 1946 and 1948, but there was an El Niño in 1943–1944. Two El Niños occurred from 1948–1955, one in 1951–1952 and another in 1953, both of moderate strength (QUINN *et al.,* 1987). Thus, the changes in depositional behavior appear to correlate with historic ENSO activity. Wind and wave directions tend to be constant throughout the annual cycle in the absence of ENSO events (*e.g.,* PIZARRO PEYRERA, 1985). ENSO-dependent variation in wind direction, incident waves, and resulting longshore currents may be the proximate cause(s) of sediment redistribution.

The data from 1955 to 1983 show the same trend already noted between 1948–1955: accretion stretching slightly north of 12 km along the baseline, and erosion along the rest of the beach-ridge plain to its northernmost point at Punta Balcones. Erosion prevailed from approximately 11 km north of the river mouth to the northern end of the plain, where the ridges coalesce. The surface area of sediment added between 1955 and 1983 was in excess of 9×10^5 m². A total of 1.33×10^6 m² of sediment was accreted in the southern portion of the Chira ridge plain between 1946 and 1983 (Figure 11). Thus, the majority of the material added to the Chira beach-ridge plain over the study period occurred between 1955 and 1983. Furthermore, the floodwaters from the 1982–1983, very strong (as classified by QUINN *et al.,* 1987) El Niño had not yet subsided when the aerial photographs used for this study were taken. Due to ENSO activity, sea level during 1982–1983 reached up to 50 cm higher than normal (ENFIELD, 1989). The amount of erosion measured between 1955 and 1983 was likely affected by the higher sea level and flooded beach-ridge plain in 1983; if so, our study underestimates the actual amount of accretion.

Piura Image Mosaics

When comparing the northwest coastal plains, the Piura ridges most closely resemble the Chira ridges in several ways, but have not yet been thoroughly studied (ORTLIEB *et al.,* 1993; RICHARDSON and MCCONAUGHY, 1987). Both the

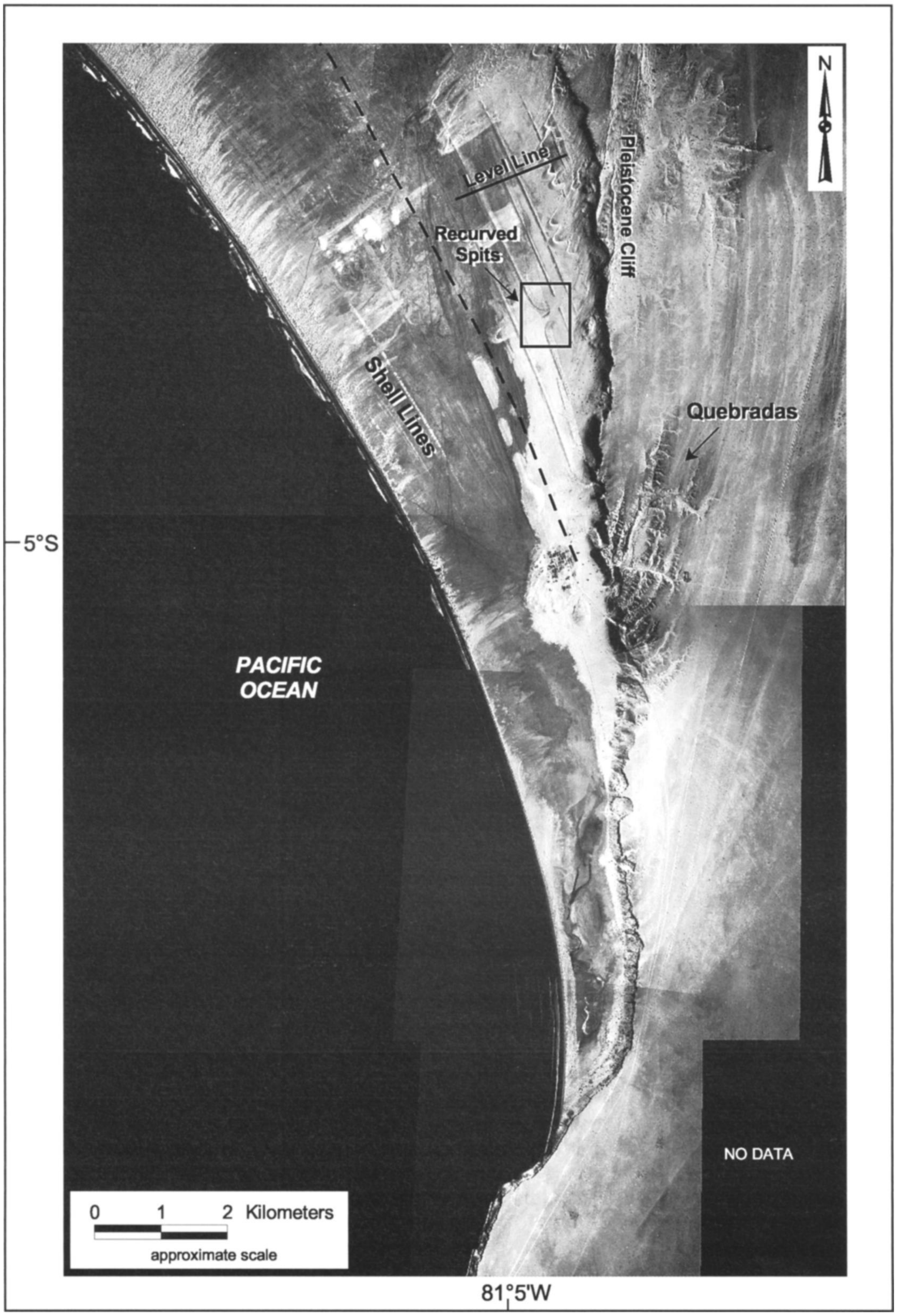

Figure 17. Colán photomosaic (1946) labeled with features referred to in text. Dashed line is the approximate shoreline position when the beach ridge source material (quebradas) was cut-off from the active shoreline. Figure 18 shows detail of the recurved spits in the box.

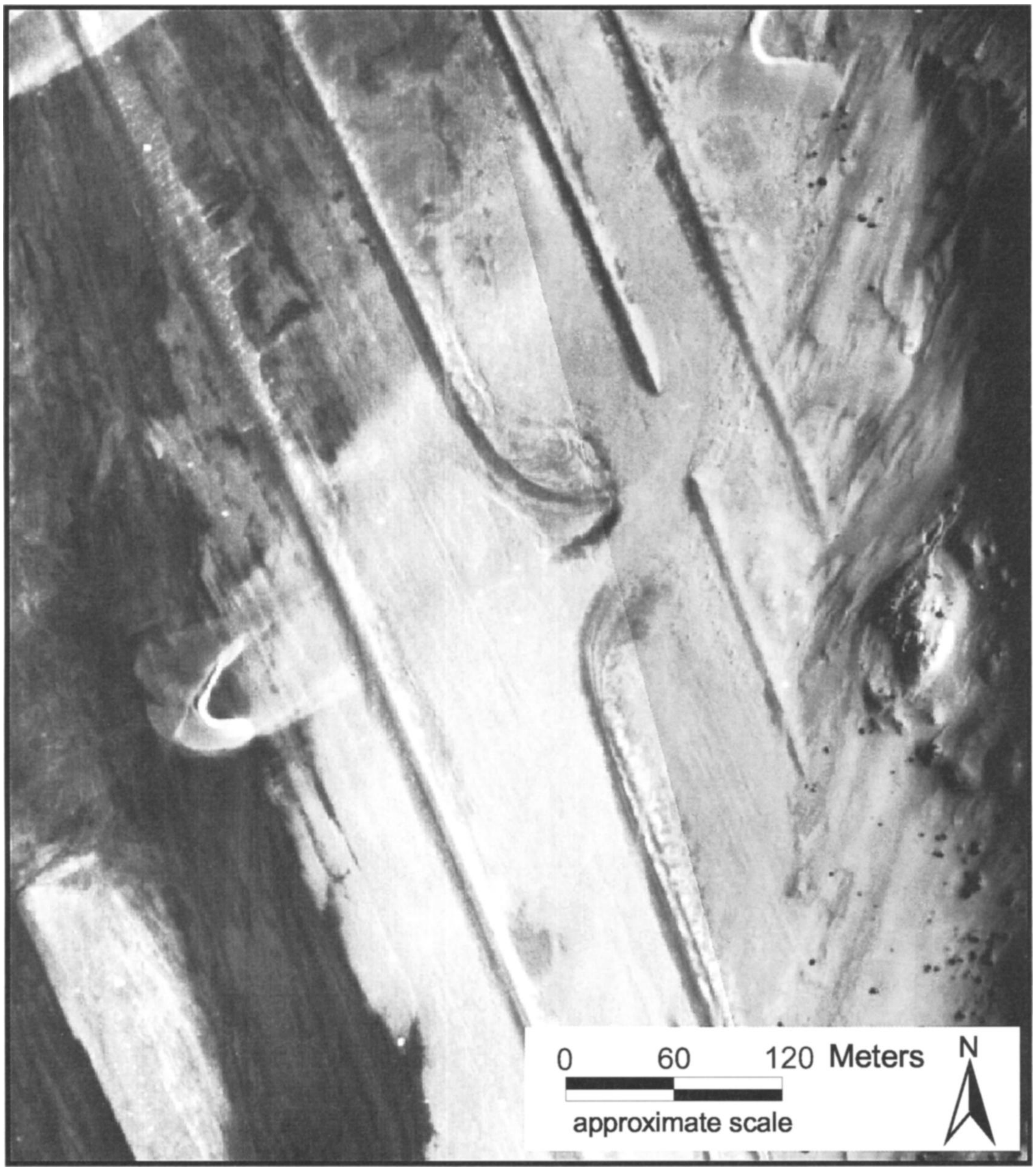

Figure 18. Recurved gravel spits at Colán.

Chira and Piura ridges are composed largely of sand and shells, however, the Piura ridges lack a continuous shell cap (Figure 12). The shell and pottery sherds present on the Piura ridges are broken and appear to have been reworked by waves. The Piura ridges are also much smaller in amplitude, attaining a maximum height from swale to crest of only 2 m compared to the 6 m height of the largest Chira ridges. The greater height of the Chira ridges is most likely due a combination of the shell cap and the competence of the Chira River, which has nine times greater discharge than the Piura (MEIGS, 1966). Wave energy levels in the Chira area may also be higher because the Chira ridge plain is exposed to the open Pacific Ocean whereas Piura is located in a more protected embayment.

The Piura ridges lack a thick shell accumulation, thus even the smaller amount of sand that was deposited in the ridges would be deflated, further reducing ridge relief and exposing any shells and pottery to wave action, especially during El Niño, when sea level is higher and torrential rains cause terrestrial flooding. However, isolated shell middens attain a height similar to the larger Chira ridges and contain large pottery sherds (LANNING, 1963, p. 142, Map 4 shows distribution of these middens). These shell middens are located near the river mouth and estuary, but are separate and dis-

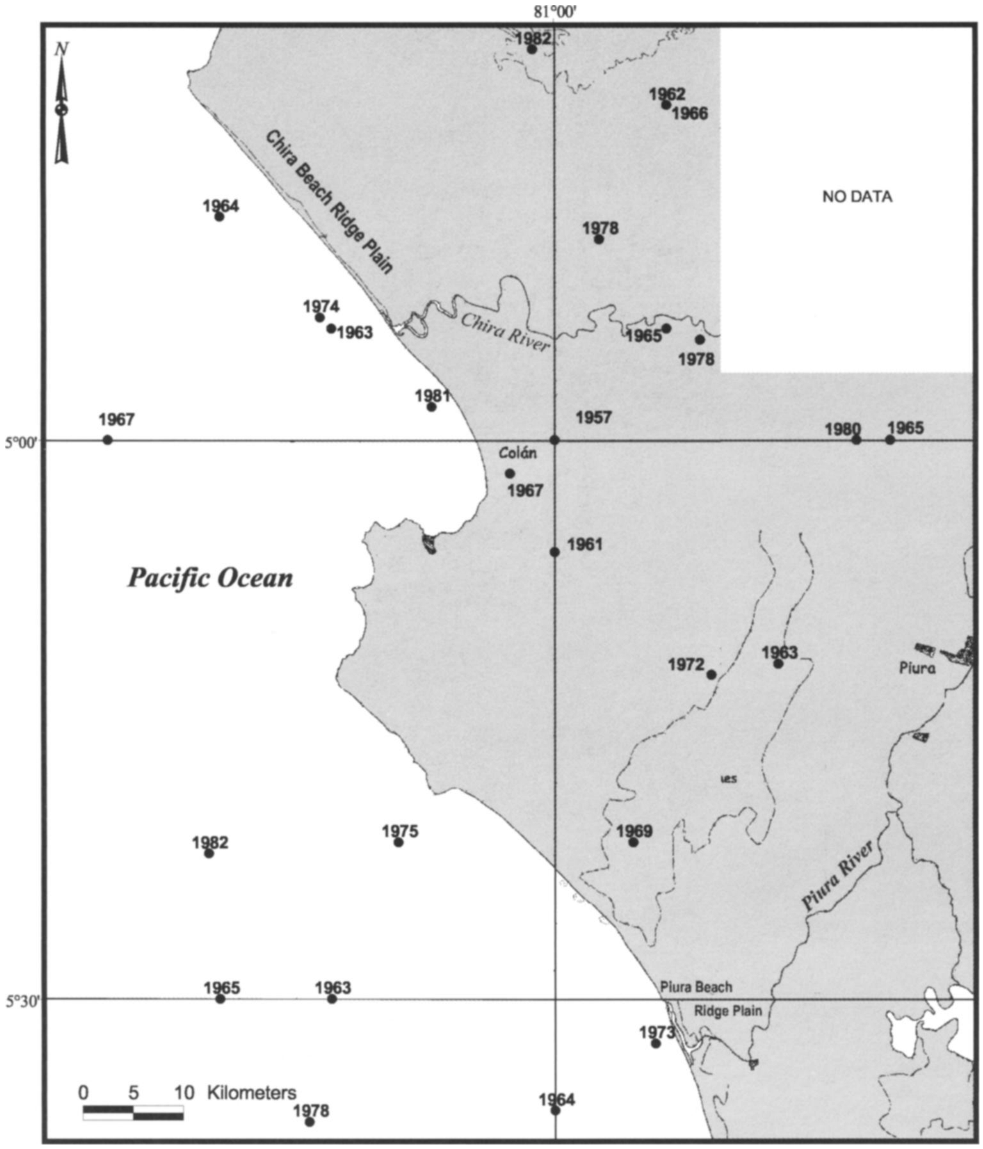

Figure 19. Earthquake epicenter locations during study period in the Chira, Colán, and Piura regions. (Data Source: ESPINOSA *et al.,* 1985).

tinct from the ridges. The aerial photographs show several shell midden mounds in a linear arrangement parallel to the ridges, but separated from each other by several tens of meters. These middens are located landward of relict river mouths at the northernmost end of the inlet. Similar shell mounds may have once existed at the mouth of earlier Piura river inlets, but were later reworked during El Niño storms into the shell hash that now composes the Piura ridges. It is unclear how much of the shell mound height is of anthropogenic origin.

The same sequence of ridges described for Chira appears to exist at Piura as well: higher ridges separated by a large swale followed by a series of smaller ridges, which become progressively smaller towards the modern shore. The oldest Piura ridges were not identified when RICHARDSON and MCCONAUGHY (1987) numbered nine Piura ridges, but only labeled the more seaward ridges. The youngest ridge now appears to be a modern sand deposit at the northern extreme of abandoned river inlets based on aerial photographic interpretation. Further interpretation of aerial photographs used for this study indicates that the newly identified landward ridges are higher than the more seaward ridges, but we did not measure them in the field (Figure 13). These initial observations suggest that the Chira and Piura coastal plains were affected by the same Holocene events, as ORTLIEB *et al.* (1993) concluded. Whether the older and larger ridges were created by a higher average sea level, a greater input of sediment, more intense El Niño storm activity or intensity, longer intervals between flood events, or any combination of these factors remains unclear.

Piura GIS Data and Analysis

A prominent characteristic of the Piura region is the rapid migration of the river inlet and reconfiguration of the southerly spit. During the study period (1946–1972) the river inlet migrated hundreds of meters north and south. This migration may be due to the constant morphological developments of the southerly spit, as it grew due to northward longshore drift and contracted due to storm erosion. Excessive amounts of sediment washed down the Piura River valley during El Niño activity could readily block the river inlet, forcing a new mouth to open as a conduit for the floodwaters.

The 1965, 1970, and 1972 aerial photo coverage of Piura displayed only the area of distinct ridge features, 7–10 km north of the river mouth. However, the 1946 and 1955 aerial photos covered 21 km, the entire length of the baseline, while the 1965–1970 data cover only 7 km of the base line length. This lack of northern coverage must be taken into consideration when comparing the total accretion and erosion change. For example, total accretion values between 1946 and 1955 at Piura are considerably greater than any other year-to-year comparison in this region due to the more complete aerial coverage.

The Piura data reflect the same trends noted in the Chira coastal change measurements: Erosion occurred along the shoreline in the midst of ENSO-related storms and increased sea level. However, within a few years following the storm cycle there was substantial accretion north of the river mouths due to sediment deposited from the flooded scoured river valleys. The newly deposited sediment appears to lead to northward shoreline accretion within a few years following an El Niño. The time period from 1955–1965 witnessed a single strong ENSO event, in 1957–1958. However, net accretion occurred over the entire interval due to a large accretionary wedge that was deposited directly north of the Piura river inlet (Figure 14). This deposit was accompanied by erosion of the spit complex directly south of river mouth, indicating that the coastline was eroded by the 1957–1958 event, but sediment was reintroduced and accretion occurred within a few years following a strong El Niño.

Two time intervals in the Piura data, 1965–1970 to 1970–1972, included El Niño events of different magnitudes. The 1972 El Niño was rated as strong by QUINN *et al.* (1987), whereas the 1965–1966 El Niño was a moderate event (M+). Tide-gauge data (PSMSL, 2002) from Talara (4°37′S, 81°17′W) suggest up to 40 cm higher-than-normal sea levels (mean monthly values) during the strong 1972–1973 El Niño, but only 16 cm higher at the peak of the 1965 event (March), and an elevation near the long-term average for October of that year. The 1965 photographs were taken on October 24th, in the middle of the 1965–1966 El Niño. However, the graph of change from 1965–1970 shows net accretion both north and south of the river mouth, indicating that the shoreline prograded within three years after the 1965–1966 El Niño (Figure 15). The 1972 images were also taken during an El Niño event, thus this interval ends in an El Niño year and is therefore dominated by erosion across the entire area of aerial coverage (Figure 16).

Colán Image Mosaic

There are eight ridges in the Colán beach-ridge sequence, located at the base of an abandoned Quaternary sea cliff (Figure 17). Closer to the modern shore there are two shell lines, which date to after 730 cal yrs BP. The beach ridges are predominately composed of gravel and smaller amounts of sand, similar to the conglomeratic material found in the cliff (ORTLIEB and MACHARÉ, 1993; ORTLIEB *et al.,* 1993; ORTLIEB *et al.,* 1995; RICHARDSON, 1983; WOODMAN and MABRES, 1993; WOODMAN and POLIA MECONI, 1974). Because El Niño rain is the only known process in this desert capable of mobilizing the cliff sediments, the release of conglomeratic material to the coastal plain for ridge creation is connected to prehistoric El Niño activity. The gravel source for the ridges is the sea cliff, however, the mode of transport for the conglomeratic material to the coastal plain is not simply cliff failure during El Niño flooding. Rather, it appears from field and aerial photo observations that the dry ephemeral stream valleys (quebradas) become activated in El Niño years and provide a point source for sediment release, much like the river valleys at other beach-ridge locations. It appears that beach-ridge formation ceases once debris flow from a quebrada can no longer reach the beachface.

We surveyed the Colán ridges, measuring a maximum relief of 3 m from crest to swale. The swales consist of fine silty sand, which is not activated by the onshore winds, indicating that there is a high water table beneath the ridge plain. The older gravel ridges do contain a limited amount of shells, many of which are unbroken. Delicate remains, such as complete sand dollars, are found within the gravelly internal structure, indicating gentle depositional processes. However, the morphology of the coastal plain at Colán has changed through time and the quebrada sources no longer supply gravel to the modern shoreline for ridge-building. At 1,000 BP the last ridge at Colán was formed before progradation cut the main source of coarse sediment off from the coastline (ORTLIEB *et al.,* 1993). It appears the shell source has remained constant. Because there is no gravel to rework, the shells are concentrated into lines instead of being intermingled with the gravel into ridges.

On the ground and from aerial photographs, the gradation of ridge size is apparent: the ridges become progressively longer through time as the size of the coastal plain increases due to progradation of sandy sediment. The quebrada source that supplied ridge material to the nearshore environment migrated southward over time. Several quebradas may run simultaneously during El Niño years, but only those that deliver gravel to the nearshore environment are a potential source for ridge-building sediment. Other material slumps at the base of the cliff backing the Colán ridges and is not available for coastal transport. Progradation rates slowed due to the regional morphology of the Colán area. Although El Niño rains still released sufficient material for ridge formation, cliff sediments were no longer deposited near the shoreline due to progradation of the coastal plain. Thus, quebrada gravels produced by later El Niño events could not be redistributed by littoral processes during non-El Niño years.

As the first eight ridges were deposited, the coastal plain

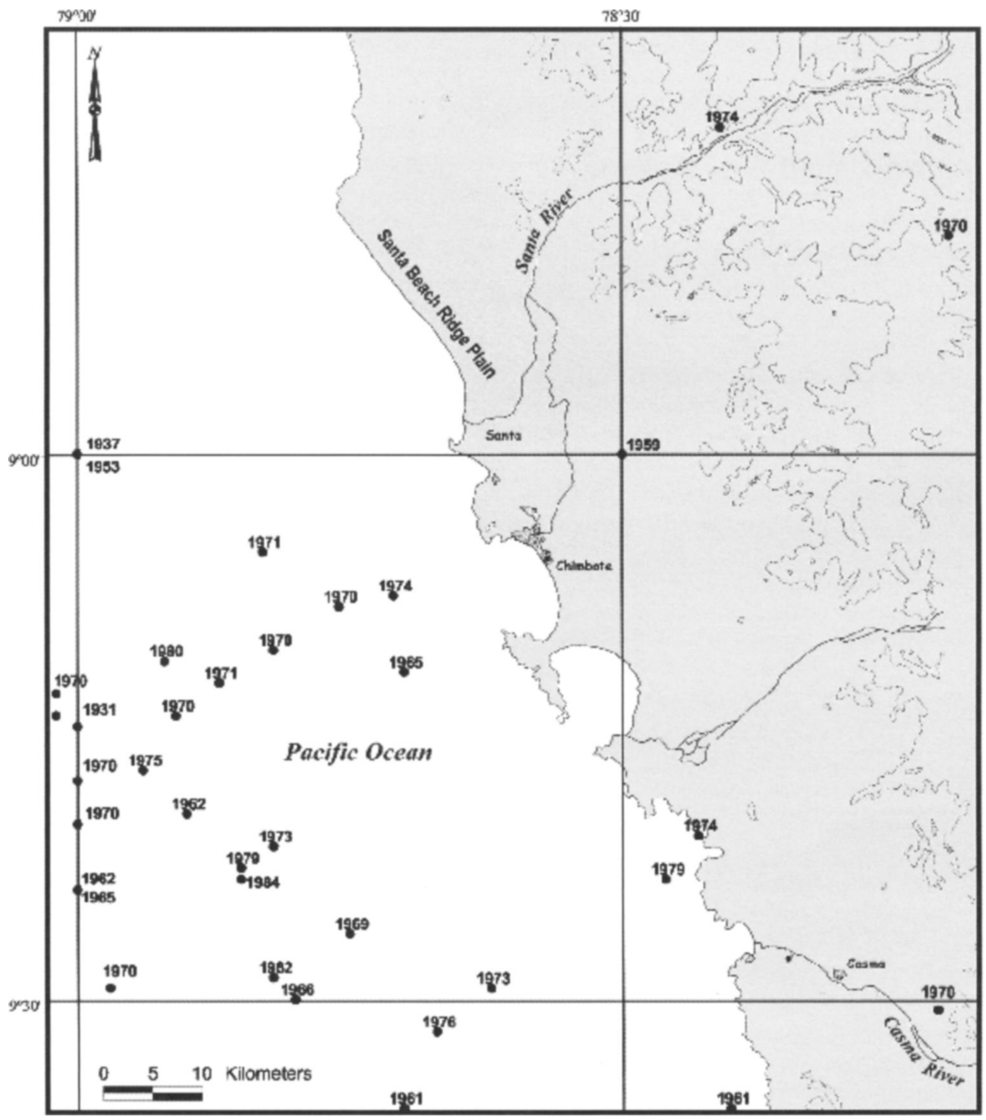

Figure 20. Earthquake epicenter locations during study period in the Santa region. (Data Source: ESPINOSA *et al.*, 1985).

prograded rapidly. Lagoons developed behind the ridges as the older ridges formed, as evidenced by the recurved gravel spits (Figure 18). The development of lagoons implies that sea level may have been higher in general when the older ridges formed. Seaward from the cliff there are three ridges; the third gently grades into a wide swale, which is approximately 200 m wide. This morphology is similar to that noted at Chira and Piura, a series of older ridges separated from the more modern ones by a considerably larger swale. However, there are a variable number of ridges on the landward side of the large swale, at Chira there are three to four ridges, while Piura has only two older ridges separated from those of more recent origin. This suggests that all three ridge sets experienced slightly different depositional events, but were generally exposed to the same climatic and environmental changes that caused a period of extremely rapid progradation.

Historic Earthquake Activity

In Peru, frequent strong earthquakes generate large volumes of landslide material from the high mountains of the Andean cordilleras to the Pacific watershed (KEEFER *et al.,* 1996; KEEFER and MOSELEY, 1994). However, most of the material may remain near its source until entrained by El Niño-induced floods (KEEFER *et al.,* 1996). The combined impact of seismic activity and El Niño flooding likely exerted exceptional stress on prehispanic Andean populations (KEEFER and MOSELEY, 1994; SATTERLEE *et al.,* 2001). The abrupt, devastating end of several prehispanic Peruvian civilizations was used to support the hypothesis of seismic-flooding impact on prehistoric peoples. For example, habitation of the Quebrada Tacahuay site in southern Peru was interrupted between 12,700 and 12,500 years ago due to catastrophic floods and debris flows, and it was not reoccupied until 3500 years ago (KEEFER *et al.,* 1998).

The May 31, 1970 earthquake epicenter 130 km off the coast of Peru affected the Santa region and provided evidence for SANDWEISS *et al.*'s (1983) seismic-El Niño hypothesis of sediment movement that may lead to beach-ridge formation (MOSELEY *et al.,* 1992). The 1970 event was the strongest earthquake in the region in over half a century: it registered 7.7 on the Richter scale and generated 1×10^8 to 2×10^8 m^3 of landslide material (PLAFKER and ERICKSEN, 1978; KEEFER and MOSELEY, 1994). Much of the material was entrained and transported to the coast by floods during 1972–1973 and 1982–1983 El Niños where it led to coastal progradation (KEEFER and MOSELEY, 1994). One of the more catastrophic effects of this earthquake was an avalanche triggered on the highest peak of the Peruvian Andes, Nevado Huascarán.

The 1970 avalanche was triggered by earthquake tremors and involved 65,000 km^2 of land in western-central Peru (PLAFKER and ERICKSON, 1978). Record rainfall in the Santa River valley during the preceding wet season had substantially loosened sediment that was activated in the avalanche (PLAFKER *et al.,* 1971). Pulses of muddy water from the debris avalanche swept down the Santa River 160 km to the sea, inundating farms and small settlements (PLAFKER *et al.,* 1971). In addition to the immediate landslides and debris flows, secondary effects took place in the coastal desert. Due to the seismic shaking, small slips on the gentle-to-moderate slopes in the saline-cemented soil crusts fragmented in a network of fine cracks, which allowed wind to activate the sand (PLAFKER *et al.,* 1971). Near-horizontal movement of liquefied water-saturated sandy deposits caused river delta and beach deposits to spread toward the shore and along river channels (PLAFKER et al., 1971). Although landslide material generated high in the Andes was likely trapped by the El Pato dam along the Santa River, material below the dam produced by secondary effects in the coastal desert would have led to substantial progradation at the Santa delta. The source of delta progradation noted by MOSELEY *et al.* (1992) may have been loosened sediment in the coastal plains and Andean foothills that was subsequently mobilized by the 1972–1973 El Niño.

During the study period all of the beach-ridge regions discussed here experienced repeated seismic activity, both offshore and in all of the headwaters. The majority of earthquake activity in the Chira, Colán, and Piura areas occurred on land, either in the region of the ridge plains or along the river valleys. In contrast, the seismic data from the Santa region revealed that most activity occurred offshore. Figures 19 and 20 display the epicenters of earthquakes that occurred along the Chira, Colán, Piura, and Santa beach-ridge sequences during the period of aerial photo coverage (1946–1983). These were plotted in the GIS from the date and coordinate data available in the U.S. Geological Survey's Earthquake Catalog of Peru (ESPINOSA *et al.,* 1985).

All beach ridge areas appear to have experienced a substantial increase in seismic activity after 1950, although the increase might be an artifact of better recording since that time. This is the same period when stronger El Niños and greater accretion occurred along the northwest Peruvian coast. No single seismic event could be singled out in correspondence to a specific instance of deposition at the river mouth or along the ridge plains (SHAFER, 1999). Rather, the earthquake data show numerous events along and around the beach-ridge regions during times of greater progradation.

CONCLUSIONS

The measurements taken from historic aerial photographs show that sediment distribution along shorelines of northwestern Peruvian ridge plains was directly affected by El Niño events. The erosion and accretion area measurements from the aerial photographs suggest that the amount of sediment that reaches the shore through the river systems is directly related to the strength of El Niño phenomena (SHAFER, 1999). Material was dispersed into both the Chira and Piura coastal environment immediately following an El Niño, and it took only a few years or less for northward progradation to occur. The image processing and GIS results show redistribution of sediment within two to five years after a moderate or strong El Niño. In time periods when El Niño was active the shoreface accreted. As the material built up at the coast it was rapidly moved away from the river mouth in the normal, non-El Niño years by northward longshore transport. El Niño activity apparently played a dual role in beach-ridge formation: initially supplying sediment to the coast by mobilizing sediment in the river valleys; then, through increased storm activity and higher sea level, allowing littoral currents to move the prograded material farther up the shoreface where it could be preserved in a ridge structure. Eventually enough sediment was accreted that the previous beach was cut off from the active coastline. Long-term supply of fluvial sediment to the littoral zone would tend to cause coastal progradation. Formation of distinct high relief and continuous ridges requires excess sediment input and/or higher wave energy from storms. Along this desert coast, both of these processes occur principally during El Niño.

Though earthquake production of loose sediment may have also played a role in ridge formation, the data and time span covered in this study did not allow us to demonstrate a direct correlation between a specific instance of seismic activity and progradation at the coastline. When seismic activity occurred, more sediment was destabilized and added to the coast through subsequent floods. The seismically loosened sediment was probably reworked and accreted together with other flood deposits at the river mouths.

Greater coastal deposition and different types of beach-ridge formation appear to be linked to late Holocene variability in El Niño frequency. Periods of ridge-building roughly coincide with blocks of hundreds of years noted around the Western Hemisphere as wetter, stormier times when ENSO activity may have been more intense. Less frequent El Niño events from 5800 to 3900 (MARTIN *et al.,* 1993) or 3000 (SANDWEISS *et al.,* 2001) cal yrs BP would have allowed more sediment to accumulate between events, before being washed to the shore by torrential El Niño rainfall. This would result in wide swales separated by larger ridges before approximately 3900 cal yrs BP After approximately 3000 cal yrs BP more frequent El Niño activity would have resulted in smaller sediment pulses separated by shorter time increments. These less intense depositional events could be moved north or seaward out of the system within a few years, as we demonstrate for recent times, as opposed to the earlier huge pulses that would have come with each widely spaced El Niño and formed large ridges. This scenario would explain the construction of two to four large ridges separated by large swales on the landward, early side of the beach-ridge plains (including Santa, SANDWEISS, 1986) and the subsequent construction of a greater number of lower amplitude ridges separated by narrower swales. The available dates are consistent with this interpretation, which in turn supports the hypothesis of changing Holocene El Niño frequency (SANDWEISS *et al.,* 2001).

This paper deals with short time-scale changes (approximately four decades) from analysis of aerial photographs. The evolution of Peruvian beach-ridge plains has occurred over five millennia. Despite this disparity in scale, we have demonstrated that short-term processes associated with ENSO provide the sediment packages necessary to form ridges, and we suggest a mechanism by which ENSO-related storm activity forms the ridges themselves. This hypothesis remains to be tested through further field research, including Ground-Penetrating Radar studies, seismic profiling, coring, and extensive radiometric dating.

ACKNOWLEDGMENTS

Image processing was conducted in the laboratories of the National Center for Geographic Information Analysis in the Spatial Information Science and Engineering Department of the University of Maine. GIS analysis was performed in the Maine Image Analysis Laboratory in the Department of Wildlife Management and Forestry. Louis Morin of the Forestry Department provided the Global Positioning System field equipment and large-format scanner used to create digital images of the paper aerial photographs. We thank James B. Richardson III and two anonymous reviewers for their useful comments on an earlier draft of this paper. We are grateful to PetroPeru, which provided housing in Talara and access to their lands. This work was funded by a NASA grant to Sandweiss and Maasch and by support for Shafer from the University of Maine Climate Change Institute (formerly the Institute for Quaternary Studies).

LITERATURE CITED

ANDRUS, C.F.T.; CROWE, D.E.; SANDWEISS, D.H.; REITZ, E.J., and ROMANEK, C.S., 2002. Otolith ^{18}O Record of Mid-Holocene Sea Surface Temperatures in Peru. *Science,* 295, 1508–1511.

ARNTZ, W.E., 1986. The two faces of El Niño 1982–1983. *Meeresforsch,* 31, 1–46.

BOSWORTH, T.O., 1922. *Geology of the Tertiary and Quaternary periods in the northwest part of Peru.* London: McMillan Company, 346p.

CROWELL, M.; LEATHERMAN, S.P., and BUCKLEY, M.K., 1991. Historical shoreline change: error analysis and mapping accuracy. *Journal of Coastal Research,* 7, 839–852.

DAVIES, J.L., 1980. *Geographical Variation in Coastal Development.* London: Longmans. 204 p.

ELY, L.L., 1997. Response of extreme floods in the southwest United States to climatic variations in the late Holocene. *Geomorphology,* 19, 175–201.

ELY, L.L.; ENZEL, Y.; BAKER, V.R., and CAYAN, D.R., 1993. A 5000-year record of extreme floods and climate change in the southwestern United States. *Science,* 262, 410–412.

ELY, L.L.; ENZEL, Y., and CAYAN, D.R., 1994. Anomalous north Pacific atmospheric circulation and large winter floods in the southwestern United States. *Journal of Climate,* 7, 977–987.

ENFIELD, D.D.B., 1989. El Niño, past and present. Reviews of Geophysics 27, 159–187.

ENFIELD, D.G., 1992. Historical and prehistorical overview of El Niño/Southern Oscillation. *In:* DIAZ, H.F. and VERA, M. (ed.) *El Niño: Historical and Paleoclimatic Aspects of the Southern Oscillation.* New York: Cambridge University Press, pp. 95–117.

ESPINOSA, A.F.; CASAVERDE, L.A.; MICHAEL, J.A.; ALVA-HURTADO, J., and VARGAS-NEUMANN, J., 1985. Earthquake catalog of Peru. *U.S. Geological Survey Open-File Report 85-286.*

JIMENEZ, J.A.; SANCHEZ-ARCHILLA, A.; BOU, J., and ORTIZ, M.A., 1997. Analysing short-term shoreline changes along the Ebro Delta (Spain) using aerial photographs. *Journal of Coastal Research,* 13(4), 1256–1266.

KEEFER, D.K.; DEFRANCE, S.D.; MOSELEY, M.E.; RICHARDSON III, J.B.; SATTERLEE, D.R., and DAY-LEWIS, A., 1998. Early maritime economy and El Niño events at Quebrada Tacahuay, Peru. *Science,* 281, 1833–1835.

KEEFER, D.K. and MOSELEY, M.E., 1994. Catastrophic effects of combined seismic landslide generation and El Niño flooding on prehispanic and modern populations in Peru. *Geological Society of America, Abstracts with Programs,* 26, 342.

KEEFER, D.K.; MOSELEY, M.E., and SATTERLEE, D.R., 1996. Recognizing seismic input in flood sediments. *Geological Society of America, Abstracts with Programs,* 28, 301.

LANNING, E.P., 1963. A ceramic sequence for the Piura and Chira Coast, North Peru. *University of California Publications in American Archaeology and Ethnology* 46(2).

LEES, B.G., 1992. Geomorphological evidence for late Holocene climatic change in northern Australia. *Australian Geographer,* 23, 1–10.

MACLEOD, R.D. and CONGALTON, R.G., 1998. A quantitative comparison of change-detection algorithms for monitoring eelgrass from remotely sensed data. *Photogrammetric Engineering and Remote Sensing,* 64, 207–217.

MARTIN, L.; FOURNIER, M.; MOURGUIART, P.; SIFEDDINE, A.; TURCO, B.; LUCIA, A.M., and FLEXOR, J.M., 1993. Southern Oscillation signal in South American palaeoclimatic data of the last 7000 years. *Quaternary Research,* 39, 338–346.

MASON, O.K., 1993. The Geoarchaeology of Beach Ridges and Cheniers: Studies of Coastal Evolution using Archaeological Data. *Journal of Coastal Research,* 9, 126–146.

MCGLONE, M.S.; KERSHAW, A.P., and MARKGRAF, V., 1992. El Niño/Southern Oscillation climatic variability in Australasian and South American paleoenvironmental records. *In:* DIAZ, H.F. and MARKGRAF, V. (ed.) *Historical and Paleoclimatic Aspects of the Southern Oscillation.* Cambridge University Press, Cambridge, Great Britain. pp. 435–462.

MEIGS, P., 1966. *The Geography of Coastal Deserts.* UNESCO: Paris. 140 p.

MOSELEY, M.E.; WARNER, D., and RICHARDSON, J.B., 1992. Space shuttle imagery of recent catastrophic change along the arid Andean coast. *In:* JOHNSON, L.L. and STRIGHT, M. (ed.) *Paleoshorelines and Prehistory: An Exploration of Method.* CRC Press: Boca Raton. pp. 215–235.

ORTLIEB, L.; FOURNIER, M., and MACHARÉ, J., 1993. Beach ridge series in Northern Peru: chronology, correlation, and relationship with major late Holocene El Niño events. *Bulletin de l'Institut Français d'Études Andines,* 22, 191–212.

ORTLIEB, L.; FOURNIER, M., and MACHARÉ, J., 1995. Beach ridges and major late Holocene El Niño events in northern Peru. *In:*

FINKL, C.W., *Journal of Coastal Research Special Issue: Holocene Cycles: Climate, Sea Levels and Sedimentation,* 17, 109–117.

ORTLIEB, L. and MACHARÉ, J., 1993. Former El Niño events: records from western South America. *Global and Planetary Change,* 7, 181–202.

PIZARRO PEYRERA, L., 1985. Comportamiento del viento superficial al Perú durante "el año" de 1982–1983. *In*: CONCYTEC, *Ciencia, Tecnología, y Agresión Ambiental: Al Fenómeno El Niño.* CONCYTEC: Lima, Peru, pp. 121–140.

PLAFKER, G. and ERICKSEN, G.E., 1978. Nevados Huascaràn avalanches, Peru. *In*: VOIGHT, (ed.). *Rockslides and Avalanches, 1 Natural Phenomena.* Amsterdam: Elsevier Scientific Publishing Company, pp. 277–315.

PLAFKER, G.; ERICKSEN, G.E., and CONCHA, J.F., 1971. Geological aspects of the May 31, 1970, Peru earthquake. *Bulletin of the Seismological Society of America,* 61, 543–587.

PERMANENT SERVICE FOR MEAN SEA LEVEL (PSMSL), 2002. Proudman Oceanographic Laboratory, UK, Web site: Talara, Peru, station 848/011.

QUINN, W.H.; NEAL, V.T., and DE MAYOLO, S.E.A., 1987. El Niño occurrences over the past four and a half centuries. *Journal of Geophysical Research,* 92, 14,449–14,461.

RICHARDSON III, J.B., 1981. Modeling the Development of Sedentary Maritime Economies on the Coast of Peru: A Preliminary Statement. *Annals of Carnegie Museum,* 50, 139–150.

RICHARDSON III, J.B., 1983. The Chira beach ridges, sea level change, and the origins of maritime economies on the Peruvian coast. *Annals of Carnegie Museum,* 52, 265–275.

RICHARDSON, J.B. and MCCONAUGHY, M.A., 1987. The Holocene beach ridges of the Chira and Piura Rivers, northwestern Peru: sea level, tectonics and El Niño. *51st Annual Meeting of the Society of American Archaeology, Toronto, Canada.*

SANDWEISS, D.H., 1986. The beach ridges at Santa, Peru: El Niño, uplift and prehistory. *Geoarchaeology,* 1, 17–28.

SANDWEISS, D.H.; MAASCH, K.; BURGER, R.L.; RICHARDSON III, J.B.; ROLLINS, H.B., and CLEMENT, A., 2001. Variation in Holocene El Niño frequencies: Climate records and cultural consequences in ancient Peru. *Geology,* 29, 603–606.

SANDWEISS, D.H.; MAASCH, K.A.; BELKNAP, D.F.; RICHARDSON III, J.B., AND H.B. ROLLINS, 1998. Discussion of The Santa Beach Ridge Complex. by Lisa E. Wells, in *Journal of Coastal Research* 12(1):1–17 (1996).

SANDWEISS, D.H.; RICHARDSON III, J.B.; REITZ, E.J.; ROLLINS, H.B., and MAASCH, K.A., 1996. Geoarchaeological evidence from Peru for a 5000 years B.P. onset of El Niño. *Science,* 273, 1531–1533.

SANDWEISS, D.H.; ROLLINS, H.B., and RICHARDSON III, J.B., 1983. Landscape alteration and prehistoric human occupation on the north coast of Peru. *Annals of Carnegie Museum,* 52, 277–298.

SATTERLEE, D.R.; MOSELEY, M.E.; KEEFER, D.K., and TAPIA, A.J.E., 2001. The Miraflores El Niño disaster: Convergent catastrophes and prehistoric agrarian change in Southern Peru. *Andean Past,* 6, 95–116.

SHAFER, S.H., 1999. Image Processing and GIS Analysis of Peruvian Beach Ridges: El Niño and Seismic Components of Coastal Change. Orono: University of Maine, M.S. Thesis, 168p.

SHULMEISTER, J. and LEES, B.G., 1995. Pollen evidence from tropical Australia for the onset of an ENSO-dominated climate at c.4000 B.P. *The Holocene,* 5, 10–18.

TAYLOR, M. and STONE, G.W., 1996. Beach ridges: a review. *Journal of Coastal Research,* 12, 612–621.

THIELER, E.R. and DANFORTH, W.W., 1994. Historical shoreline mapping (I): improving techniques and reducing position errors. *Journal of Coastal Research,* 10, 549–563.

TUDHOPE, A.W.; CHILCOTT, C.P.; MCCULLOCH, M.T.; COOK, E.R.; CHAPPELL, J.; ELLAM, R.M.; LEA, D.W.; LOUGH, J.M., and SHIMMIELD, G.B., 2001. Variability in the El Niño-Southern Oscillation through a Glacial-Interglacial Cycle. *Science,* 291, 1511–1517.

WELLS, L.E., 1987. An alluvial record of El Niño events from northern coastal Peru. *Journal of Geophysical Research,* 92, 14,463–14,470.

WELLS, L.E., 1988. Holocene fluvial and shoreline history as a function of human and geologic factors in arid northern Peru. Stanford University, Unpublished Thesis doctoral dissertation, 396p.

WELLS, L.E., 1990. Holocene history of the El Niño phenomenon as recorded in flood sediments of northern coastal Peru. *Geology,* 18, 1134–1137.

WELLS, L.E., 1996. The Santa beach ridge complex: sea level and progradational history of an open gravel coast in central Peru. *Journal of Coastal Research,* 12, 1–17.

WOODMAN, R.F. and MABRES, A., 1993. Formacion de un cordon litoral en Mancora, Peru, a raiz de El Niño de 1983. *Bulletin de l'Institut Francais d'Études Andines,* 22, 213–226.

WOODMAN, R.F. and POLIA MECONI, M., 1974. Evidencia arqueológica del levantamiento continental al norte del Perú en los últimos 4 mil años. *Boletín de la Sociedad Geográfica de Lima,* 93, 63–66.